

International
Progress Report

IPR-99-12

Äspö Hard Rock Laboratory

TRUE 1st Stage Tracer test programme

Tracer tests with sorbing tracers, STT-1b

Experimental description and preliminary evaluation

Peter Andersson, Eva Wass
GEOSIGMA

Henrik Johansson, Gunnar Skarnemark, Mats Skålberg
Department of Nuclear Chemistry, Chalmers

May 1999

Svensk Kärnbränslehantering AB

Swedish Nuclear Fuel
and Waste Management Co
Box 5864
SE-102 40 Stockholm Sweden
Tel 08-459 84 00
+46 8 459 84 00
Fax 08-661 57 19
+46 8 661 57 19



**Äspö Hard Rock
Laboratory**

Äspö Hard Rock Laboratory

TRUE 1st Stage Tracer test programme

Tracer tests with sorbing tracers, STT-1b

Experimental description and preliminary evaluation

Peter Andersson, Eva Wass
GEOSIGMA

Henrik Johansson, Gunnar Skarnemark, Mats Skålberg
Department of Nuclear Chemistry, Chalmers

May 1999

Keywords: TRUE-1, tracer test, sorbing tracers

This report concerns a study which was conducted for SKB. The conclusions and viewpoints presented in the report are those of the author(s) and do not necessarily coincide with those of the client.

Abstract

This report describes the performance and evaluation of the second tracer test with radioactive sorbing tracers (STT-1b) within the TRUE-1 project. The test was performed in the detailed scale at the TRUE-1 site, Äspö HRL, with the main objective to test equipment and procedures for tests with radioactive sorbing tracers to be performed in later stages of the TRUE Project. The test also aimed at increasing the understanding of transport and retention of sorbing species in crystalline rock and obtaining in situ data of sorption from yet another flow path within the selected water conducting structure denoted Feature A.

STT-1b was made by injecting four conservative (non-sorbing) and six sorbing tracers in a radially converging flow geometry over a distance of 5 m within Feature A. Breakthrough from nine of the ten tracers was detected in the pumping section. Numerical modelling using a simple one-dimensional transport model with advection, dispersion and linear sorption, showed that the breakthrough of conservative tracers (Uranine, HTO, ^{82}Br and ^{131}I) and the weakly sorbing tracers ^{22}Na and ^{85}Sr could be relatively well simulated. The breakthrough curves for the moderately sorbing tracers ^{86}Rb and ^{58}Co could not be well fitted, especially in the tail of the breakthrough curves indicating that additional processes are needed to explain the breakthrough.

The tailing of the breakthrough curve for ^{137}Cs from the injection in another flow path in the previous sorbing tracer test STT-1 was followed also during STT-1b. Model runs was made using breakthrough data for the longer test period and the new model parameters differ somewhat from the previous ones reported in Andersson et al., 1998. Values of mean travel time, dispersivity and retardation coefficient are higher using the extended breakthrough data set.

Executive Summary

This report describes the performance and preliminary evaluation of the second TRUE-1 tracer test with sorbing tracers, STT-1b. The test was performed in the detailed scale (<10 m) within Feature A at the TRUE-1 site at the Äspö HRL.

The main objective for the tests with sorbing tracers was to test equipment and procedures for tests with radioactive sorbing tracers to be performed in later stages of the TRUE Project. Secondly, to increase the understanding of transport and retention of sorbing species in crystalline rock and to obtain in situ sorption data.

STT-1b was performed in Feature A in a radially converging flow geometry between boreholes KXTT1 R2 → KXTT3 R2. In total ten tracers, four conservative (Uranine, tritiated water, ^{82}Br and ^{131}I) and six weakly to moderately radioactive sorbing tracers (^{22}Na , ^{42}K , ^{85}Sr , ^{86}Rb , ^{58}Co and $^{99\text{m}}\text{Tc}$) were mixed and injected as a finite pulse with a duration of four hours. Tracer breakthrough in the pumping section was monitored for all tracers injected, except $^{99\text{m}}\text{Tc}$. The breakthrough curves show one high and distinct single peak with much less tailing than observed during STT-1, possibly due to a more efficient tracer exchange procedure resulting in a well-defined end of the finite injection pulse.

The experimental set-up for STT-1b was, with some minor modifications, identical to the one used in STT-1 (Andersson et al., 1998) and PDT-3 (Andersson & Wass, 1998). The tracer exchange (ending of the finite tracer pulse) during STT-1 was not very efficient, therefore the exchange procedure was repeated twice during STT-1b. The removal of tracer solution gave a reduction of about 95 % of the mass in the tracer injection loop. This reduction is still too small to avoid that the slow release of the remaining tracer solution potentially may mask important transport processes in the breakthrough curve. A redox probe was also installed in the sampling loop for the withdrawn water due to the use of the redox-sensitive tracer $^{99\text{m}}\text{Tc}$.

The injection procedure, during which the highest doses of radioactivity could be expected, was performed with very low doses to the personnel. The activity of the water discharged into the tunnel only showed a temporary increase relative to the background activity during the peak of the breakthrough.

The evaluation of tracer mass recovery showed some inconsistencies. Calculated mass recoveries based on integrated mass fluxes were found to be more than 100 % and differ considerably from tracer mass values calculated based on weighing and concentration measurements from the exchange procedure. Based on earlier tests and uncertainties in the weighing and concentration measurements, the values determined by integration of the injection and breakthrough curves, corrected by assigning a larger (28 %) volume to the injection section, were considered to be the most appropriate to use.

The flow path KXTT1 R2 → KXTT3 R2 has earlier been tested in several different experiments. The values of transport parameters determined from STT-1b are similar to

those determined from PTT-1 (Winberg *et al.*, 1996) and RC-1 (Andersson, 1996) which are the most appropriate values to compare with although the pumping rates were different. The remaining three tests (DP-1, PDT-1 and PDT-2) were performed with lower pumping rates, giving less mass recovery and somewhat deviating parameter values.

A comparison of the flow rate in the injection section KXTT1 R2 during RC-1 and STT-1b shows a significant increase from 44 to 58 ml/h (compensated for the increased volume in the section). This is also consistent with the observations from STT-1 for the injection interval KXTT4 R3 (Andersson *et al.*, 1998). The measured flow is about a factor 10 higher than the background flow (5 ml/h) measured in April 1997 (Andersson & Wass, 1997) and represents a contribution corresponding to three borehole diameters, which is not far from the theoretical homogeneous porous case of two borehole diameters.

The increasing flow rate in the injection section and the increasing head difference between pumping and injection sections indicate a non-stationary flow field at the TRUE-1 site over the duration of the performed tracer test. The reason for these changes may be effects of hydraulic boundaries during this long-term pumping (8 months). Another explanation may be changes in the local transmissivity around the sections caused by chemical clogging, bacterial growth, etc.

The transport of the radioactive sorbing tracers showed significant retardation for all tracers. The retardation coefficients determined from a simple linear surface sorption model were found to vary between $R=1.4$ for ^{22}Na to $R=57$ for ^{58}Co .

The utilised numerical model worked reasonably well for the simultaneous fit of the conservative tracer breakthrough (Uranine) and one of the weakly sorbing tracers ^{22}Na or ^{85}Sr . However, the fits using Uranine and the moderately sorbing tracers ^{86}Rb or ^{58}Co , individually, were not good, especially in the tail part of the breakthrough curves. Thus, the linear surface sorption process alone cannot explain the retardation of these species.

The tailing of the breakthrough curve for ^{137}Cs from the injection in the previous sorbing tracer test STT-1 in the flow path KXTT4 R3 \rightarrow KXTT3 R2, was followed also during STT-1b. The recovered mass for ^{137}Cs at the end of the extended test period was 33 %. Model runs were made using breakthrough data for the longer test period and the new model parameters differ somewhat from the previous ones reported in Andersson *et al.*, 1998. Values of mean travel time, dispersivity and the retardation coefficient are higher using the extended breakthrough data set.

Contents

| | |
|---|-----------|
| Abstract | i |
| Executive Summary | ii |
| Contents | iv |
| 1 Introduction | 1 |
| 1.1 Background | 1 |
| 1.2 Objectives | 1 |
| 2 Experimental set-up | 2 |
| 2.1 Equipment and tracers used | 2 |
| 2.1.1 Borehole equipment | 2 |
| 2.1.2 Injection equipment | 2 |
| 2.1.3 Sampling and detection equipment | 4 |
| 2.1.4 Tracers used | 5 |
| 2.2 Injection Procedure | 5 |
| 2.3 Sampling and detection procedures | 5 |
| 2.4 Environmental sampling and control | 7 |
| 3 Results | 9 |
| 3.1 Performance of pre-test PDT-4 | 9 |
| 3.1.1 Objective | 9 |
| 3.1.2 Performance | 9 |
| 3.1.3 Results | 9 |
| 3.2 Log of events | 11 |
| 3.3 Tracer injections | 11 |
| 3.4 Tracer breakthrough | 15 |
| 3.4.1 Tracer breakthrough data interpretation | 15 |
| 3.4.2 Numerical modelling | 19 |
| 3.4.3 Tracer mass recovery | 28 |
| 3.4.4 Cs-137 from STT-1 | 29 |
| 3.5 Supporting data | 31 |
| 4 Discussion and conclusions | 34 |
| 4.1 Experimental set-up and performance | 34 |
| 4.2 Flow and transport in Feature A | 35 |
| 5 References | 38 |

Appendix A

Tracer breakthrough data (log-log scale) and injection data (Uranine, log-log scale) from STT-1b and Cs-137 from STT-1.

1 Introduction

1.1 Background

A programme has been defined to increase the understanding of the processes that govern retention of radionuclides transported in crystalline rock, the Tracer Retention Understanding Experiments (TRUE). The basic idea is to perform a series of tracer tests with progressively increasing complexity.

The first tracer test cycle (TRUE-1) constitutes a development stage for tracer testing technology on a detailed scale using conservative and sorbing tracers in a simple test geometry. In addition, supporting technology development is performed for understanding of tracer transport through detailed aperture distributions obtained from resin injection, and for sampling and analysis techniques for matrix diffusion.

So far, a number of tracer tests have been performed in a selected water conducting structure, Feature A, using non-sorbing (conservative) tracers namely; Preliminary Tracer Tests, PTT (Winberg (*ed*), 1996), Radially Converging Tracer Test, RC-1 (Andersson, 1996), Dipole Tracer Tests, DP-1 - DP-4 (Andersson et al., 1997b) and Complementary Tracer Tests, RC-2, DP-5 - DP-6 (Andersson & Jönsson, 1997). A number of preparatory tests for the sorbing tracers tests have been performed including a series of dilution tests (Andersson & Wass, 1997) and three tracer tests in radially converging flow geometry, PDT-1 - PDT-3 (Andersson & Wass 1998).

Since July 1997 the first tracer test with sorbing tracers, STT-1 (Andersson et al., 1998), has been under-way. The resulting tracer breakthrough showed a long tailing of the ^{137}Cs breakthrough. It was therefore decided to follow the tail of the ^{137}Cs breakthrough until March 1998 and to include a second complementary injection of sorbing tracers in another flow path within Feature A.

This report describes the results and preliminary evaluation of this second tracer injection with sorbing tracers, STT-1b, at the TRUE-1 site.

1.2 Objectives

The overall objective for the tests with sorbing tracers was to test equipment and procedures for tests with radioactive sorbing tracers to be performed in later stages of the TRUE Project. Secondly, to increase the understanding of transport and retention of sorbing species in crystalline rock. The purpose of STT-1b was to obtain in situ data of sorption from yet another flow path within Feature A.

2 Experimental set-up

2.1 Equipment and tracers used

2.1.1 Borehole equipment

Each borehole in the TRUE-1 array is instrumented with 4-5 inflatable packers such that 4-5 borehole sections are isolated. All isolated borehole sections are connected to the Äspö HRL Hydro Monitoring System (HMS) through data loggers (Borre 6). Each of the sections planned to be injection or sampling sections are equipped with three nylon hoses, two with an inner diameter of 4 mm and one with an inner diameter of 2 mm. The two 4-mm hoses are used for injection, sampling and circulation in the borehole section whereas the 2-mm hose is used for pressure monitoring.

The borehole sections in Feature A are also equipped with volume reducers (dummies) and a perforated tube, cf. Andersson (1996). The perforated tube and dummies are important prerequisites to achieve a complete and fast homogenisation of the tracer solution added to the system. The volume reduction of the system, including tubing, due to the dummies is about 40 % for a 1-m section length and 60 % for a 2-m section.

2.1.2 Injection equipment

A schematic drawing of the tracer injection equipment is shown in Figure 2-1. The basic idea is to create an internal circulation of the borehole fluid in the injection borehole. The circulation makes it possible to obtain homogeneous tracer concentration inside the borehole and to sample the tracer concentration outside the borehole in order to monitor the dilution of the tracer with time.

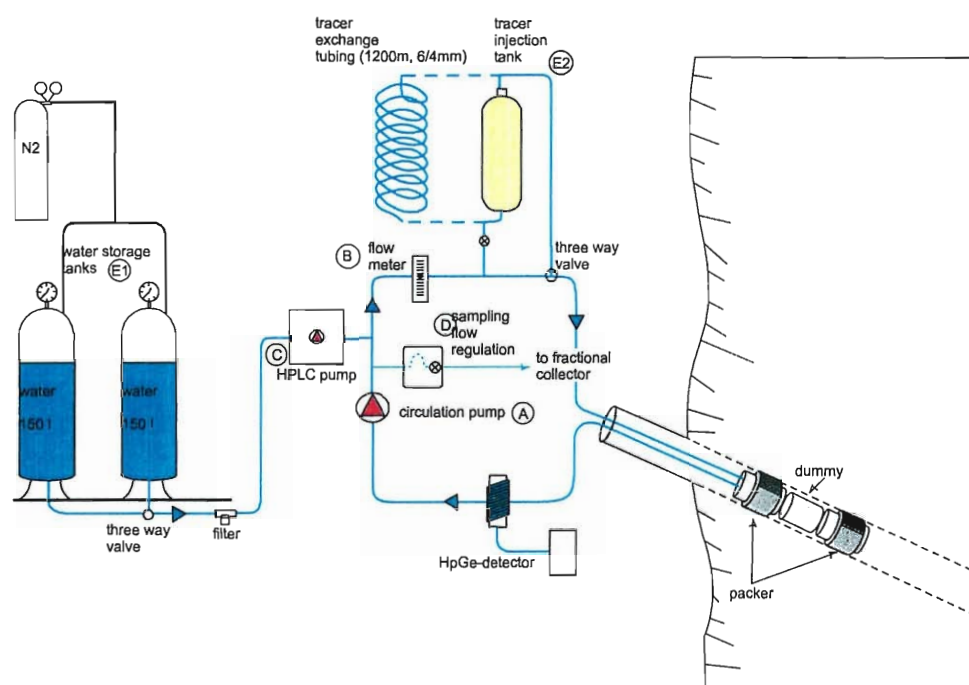


Figure 2-1. Schematic drawing of the injection system for the TRUE-1 tracer tests with sorbing tracers.

Circulation is controlled by a pump with variable speed (A) and measured by a flow meter (B). Tracer injections are made either directly into the circulating loop with a HPLC plunger pump (C) or by switching a three-way valve so that the circulating water passes through a stainless steel vessel (E2) filled with tracer solution. Thus, unlabelled water from the circulation loop enters the bottom of the vessel and tracer labelled water enters the circulation loop from the top of the vessel. The three-way valve is then switched back again after replacing the volume of the vessel. The tracer solution in the circulation loop can also be replaced with unlabelled water by switching the three-way valve so that the circulating water passes through a long (1200 m) tube filled with unlabelled water. Tracer solution then enters from one side of the tube and unlabelled water enters the circulation loop from the other side of the tube.

The tracer concentration in the injection loop is measured both in situ and by sampling and subsequent analysis. The sampling is made by continuously extracting a small volume of water from the system through a flow controller (constant leak) to a fractional sampler (D). The in-situ monitoring of tracer content in the injection system (source term) is made with a HPGe-detector measuring in-line on the tubing.

Water from Feature A used for the tracer exchange is stored in a separate pressurised vessel (E1) under nitrogen atmosphere. Further details about the equipment are given in Andersson, (1996).

2.1.3 Sampling and detection equipment

The sampling system is based on the same principle as the injection system, namely a circulating system with a circulation pump and a flow meter, cf. Figure 2-2. In this case however, water is withdrawn from the borehole with a constant flow rate by means of a flow regulation unit. This unit consists of a mass flow meter coupled to a motorised valve enabling a fast and accurate flow regulation.

The sampling is made with two independent systems, a "constant leak" system producing 8 ml samples (same as the injection loop) integrated over some time (5-100 minutes) and a 24-valve sampling unit producing discrete 1 litre samples.

After sampling, the pumped water is led through a redox potential probe and further through a nylon vessel where the water is degassed. The reason for degassing is that measurement of dye tracer content is made by an in line field fluorometer. As fluorometry is an optical method, gas bubbles need to be removed in advance otherwise they will create a fictive background content of the dye tracer. Hence, the degassed water is pumped from the degassing vessel through the field fluorometer and further through an electrical conductivity probe.

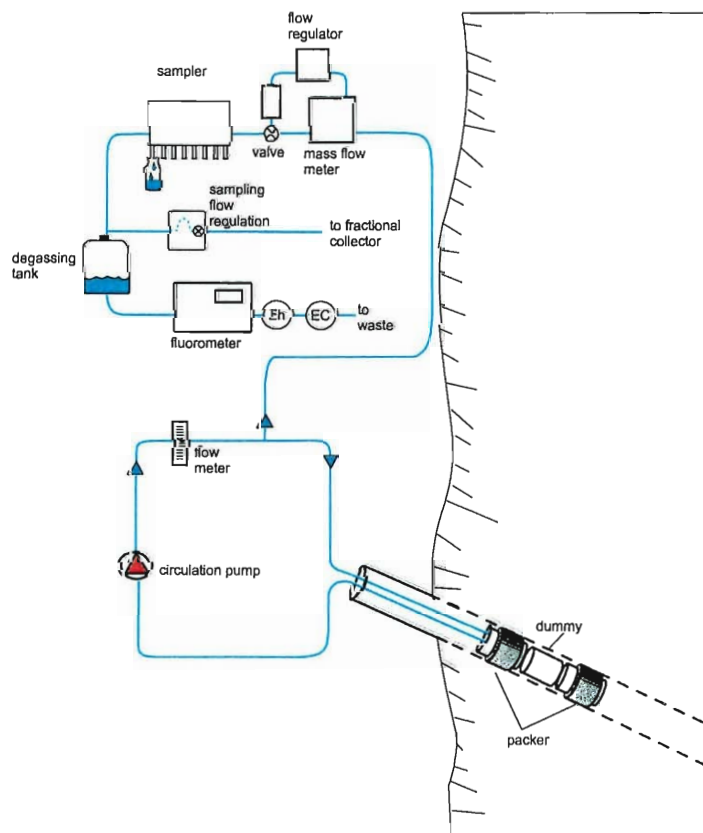


Figure 2-2. Schematic drawing of the sampling system for the TRUE-1 tracer tests with sorbing tracers.

2.1.4 Tracers used

During STT-1b, a mix of totally ten different tracers, both conservative and sorbing, was injected. The sorbing tracers used were six radioactive, gamma-emitting, isotopes of mono- and divalent cations, cf. Table 3-3. These tracers needed to be injected in such low concentrations that the chemical conditions were kept unchanged in Feature A. Another restriction was the maximum permitted dose. The conservative tracers used were Uranine (Sodium Fluorescein), tritiated water (HTO) and the radioactive tracers ^{82}Br and ^{131}I . The equipment was also tested for sorption of the tracers used in STT-1b and no significant sorption could be detected, cf. Ittner & Byegård (1997).

2.2 Injection Procedure

A tracer solution (3 litres) containing all ten tracers was prepared at SKB BASLAB. The radionuclides were dissolved in de-ionised water and mixed into a tracer stock solution with H^3HO (HTO) and Uranine that were used as the base conservative tracers. The stock solution was pH-adjusted to ~ 7.5 by addition of diluted NaOH. A sample was taken before transport of the stock solution to the experimental site. After transport to the TRUE-1 site the tracer solution was pumped from the transport vessel into the stainless steel injection tank using a peristaltic pump. Non-traced water (about 1.5 litre) was added from the water storage vessel to fill the injection tank completely. The injection tank was pressurised by adding water with the HPLC injection pump until the injection section pressure was reached. The three-way valve in the injection loop was then switched to start the tracer injection, cf. Figure 2-1.

The injection of tracer was performed as a finite pulse injection with a length of four hours. After four hours of injection the tracer solution was exchanged with unlabelled water as described in Chapter 2.1.2. The exchange procedure lasted 60 minutes. A second exchange was made 100 minutes after the end of the first one to achieve an even more efficient exchange ($>90\%$) and it lasted for 25 minutes.

The recovered tracer solution was stored in the exchange tubing and in plastic vessels for subsequent measurement of recovered mass.

2.3 Sampling and detection procedures

Both the injection concentrations (activities) and the concentrations in the pumped water were monitored using the equipment described in Chapter 2.1.2 and 2.1.3. The decrease in injection concentration was measured by sampling for Uranine and HTO with samples taken every 2nd minute during the initial 36 minutes of injection and then every 30 minutes up to 4 hours. The sampling frequency was then increased again to every 2nd minute during the first exchange from four to five hours. After this period samples were taken once every hour until the second exchange started. During the second exchange

the sampling frequency was increased to every 4th minute from 5 to 5.4 hours and afterwards once every hour gradually decreasing to a sample every fifth hour.

During the tracer injection, the radioactivity was measured by on-line γ -spectroscopy using a HPGe-detector (25 % relative efficiency, EG&G ORTEC, USA). The volume of the injection loop tube passing the detector at a distance of ~ 1 cm was ~ 1 ml and the detector was calibrated using a tube filled with a mixed radionuclide standard (Amersham QCY44). The radionuclides were measured with the in line detector with a somewhat higher frequency than the discrete sampling during the first ten hours. After this period activity measurements were made over a period of one hour.

The sampling in the pumping borehole was performed using the two independent sampling systems described in Chapter 2.1.3. Both systems were set to take samples once every 10th minute during the first two hours. The sampling frequency was then increased to one sample every 5th minute during the next two hours and then gradually decreasing to one sample per day after a month.

The samples were stored in special transport cases and transported to SKB BASLAB for analysis. The samples were subsequently split up and treated in different ways depending on the analysis method to be employed. A flow chart describing the different treatment and analysis steps at BASLAB is shown in Figure 2-3.

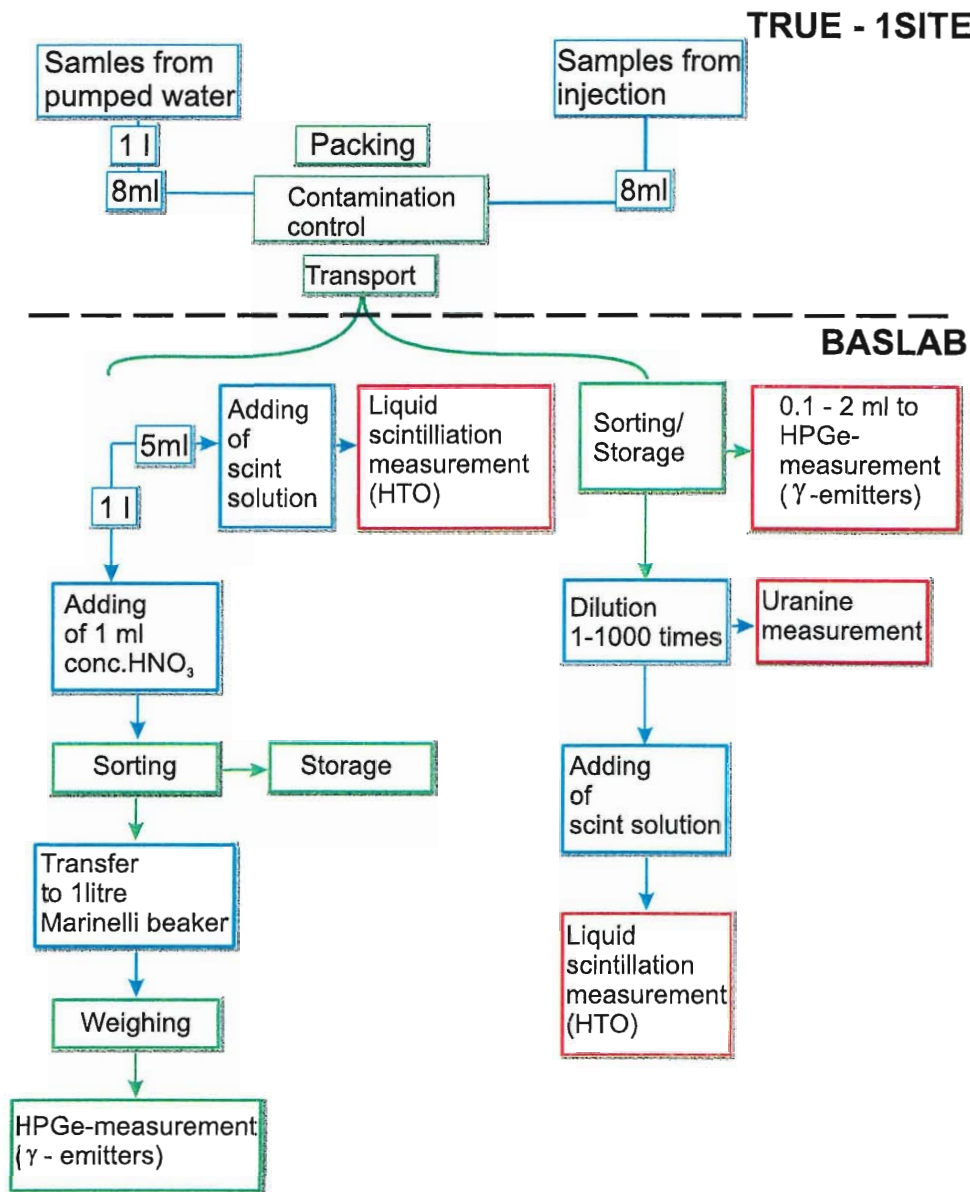


Figure 2-3. Schematic drawing of the handling and analysis of samples from STT-1b at BASLAB.

2.4 Environmental sampling and control

Besides measuring samples from the TRUE-1 experimental site, environmental samples have been taken regularly from six strategic places in the tunnel to monitor potential leakage/spills. In addition, a gamma detector was installed in the tunnel weir to which the drainage from the experimental site is connected, located at tunnel length 3/020 m. The detector was connected to the Äspö data network allowing continuous monitoring. The radiation levels are shown in Figure 2-4, where levels are given in counts per

second (cps). During the breakthrough from STT-1b an increase from 20 cps (background level) to 40 cps can be seen. The second peak measured on December 21st represents the breakthrough of ^{58}Co . A sample taken in the weir on December 5th and analysed at BASLAB shows activities of HTO of about 60 Bq/l, ^{22}Na 1.3 Bq/l and ^{85}Sr 0.6 Bq/l. The activities of the other nuclides were below detection limits. No non-natural radioactivity has been detected in the other environmental samples.

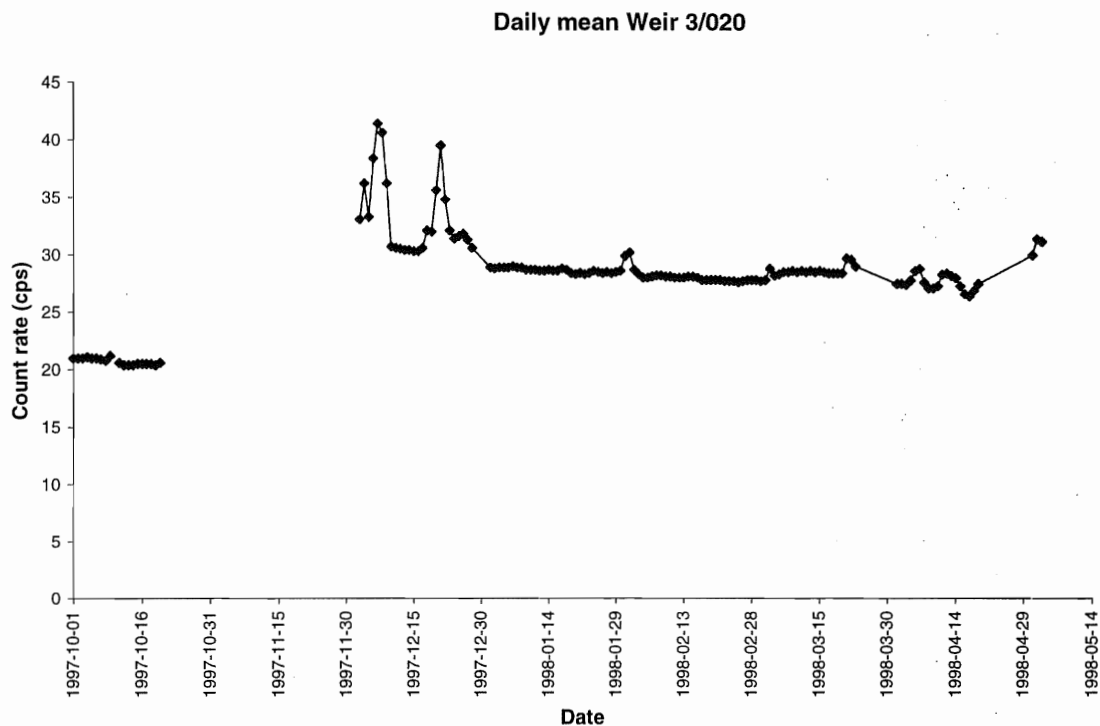


Figure 2-4. Daily mean values of radiation level (counts per second) in the tunnel weir at 3/020 m during STT-1b.

3 Results

3.1 Performance of pre-test PDT-4

3.1.1 Objective

The flow path KXTT1 R2 has earlier been tested in several different flow geometries (RC-1, DP-1, PDT-1 and PDT-2), cf. Table 4-1. However, the last test performed, PDT-2, showed an incomplete recovery of tracer at the pumping rate 200 ml/min in KXTT3 R2 (Andersson & Wass, 1998). Therefore, a preliminary design test was performed to check the tracer recovery at a pumping rate at 400 ml/min.

The purpose of the preliminary design test, PDT-4, was to optimise test procedures for STT-1b and also to check that tracer mass recovery of the selected flow path was high.

3.1.2 Performance

The injection of tracer was performed as a finite pulse injection with a length of three hours. After three hours of injection the tracer solution was exchanged with unlabelled water as described in Chapter 2.1.2. The exchange procedure lasted 90 minutes. Sampling in the injection section was made by a “constant leak” system.

In the sampling section, KXTT3 R2, tracer breakthrough measurements was made using a field fluorometer in-line on the tubing together with the “constant leak” sampling system as described in Chapter 2.1.3.

All samples were analysed at BASLAB.

3.1.3 Results

The injection and breakthrough curves of PDT-4 are shown in Figure 3-1. Four time periods with somewhat different injection flow rates were identified, cf. Table 3-1. Due to a higher uncertainty in the calculated value for the first time period (0-3 h) indicated by the low correlation coefficient for the straight-line fit, the flow calculated for 12-44 hours was also used for the time period 0-12 hours. A comparison can be made with the injection flow rates determined for STT-1b, cf. Table 3-4, where flow rates of 50-60 ml/h were calculated for the time period after the tracer exchanges.

Tracer mass recovery was calculated by integration of the injection and breakthrough curves. The recovery for Uranine in PDT-4 was 78 % after 137 hours of sampling. Even

though it was not as high as expected it was considered high enough for STT-1b to be performed.

Table 3-1 Injection flow rates at different time periods during PDT-4 calculated from the dilution of Uranine. R is the correlation coefficient for the straight line fit.

| Time period (h) | Flow (ml/h) | R |
|-----------------|-------------|--------|
| 0-3 | 14.7 | 0.5742 |
| 12-44 | 37.6 | 0.9949 |
| 44-80 | 50.2 | 0.9987 |
| 80-150 | 61.7 | 0.9999 |

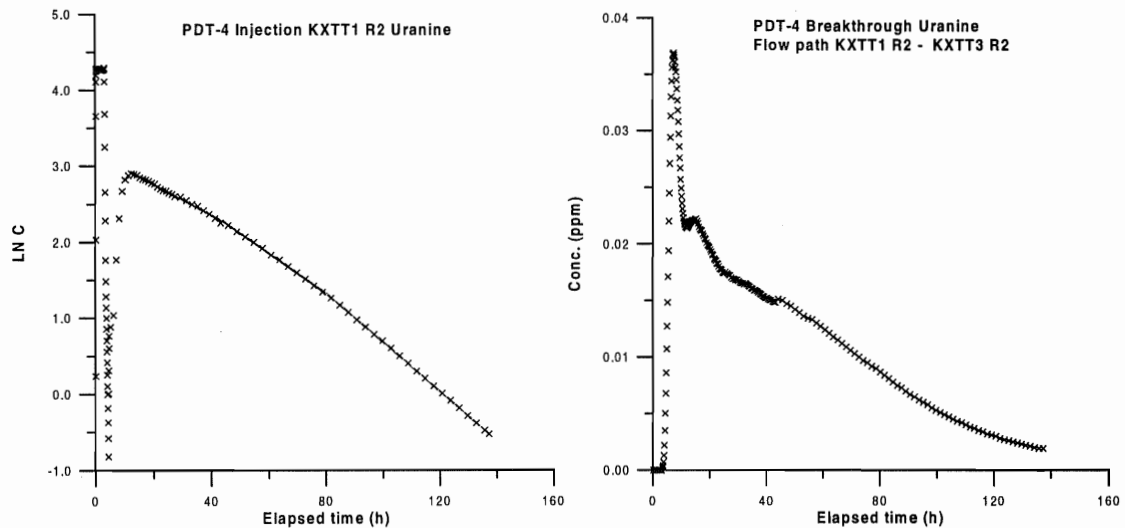


Figure 3-1 a) Tracer injection concentration ($\ln C$) versus elapsed time, t (h) for Uranine in the injection section KXTT1 R2 during PDT-4. b) Tracer breakthrough concentration (ppm) versus elapsed time, t (h) for Uranine in the pumping section KXTT3 R2 during PDT-4.

3.2 Log of events

The test period described in this report lasted between November 19th, 1997 and May 3rd, 1998.

Table 3-2 Log of events during PDT-4 and STT-1b.

| Date | Time | Event |
|--------|-------|---|
| 970612 | 13.30 | Start pumping in KXTT3 R2, Q=0.400 l/min |
| 971119 | 17.10 | Start tracer injection KXTT1 R2 (PDT-4) |
| 971119 | 20.10 | Start water injection (removal of tracer solution) in KXTT1 R2 (PDT-4) |
| 971119 | 21.40 | Stop water injection in KXTT1 R2 (PDT-4) |
| 971203 | 14.10 | Start tracer injection KXTT1 R2 (STT-1b) |
| 971203 | 18.10 | Start water injection (removal of tracer solution) in KXTT1 R2 (STT-1b) |
| 971203 | 19.10 | Stop water injection in KXTT1 R2 (STT-1b) |
| 971203 | 20.50 | Start water injection (removal of tracer solution) in KXTT1 R2 (STT-1b) |
| 971203 | 21.15 | Stop water injection in KXTT1 R2 (STT-1b) |

3.3 Tracer injections

The ten tracers injected during STT-1b are listed in Table 3-3 together with the maximum concentrations measured in the injection loop. The decrease in concentration versus time was used to calculate the flow rates through the borehole by plotting the natural logarithm of concentration versus time. Theoretically, a straight-line relationship exists between the natural logarithm of the relative tracer concentration (C/C_0) and time (t):

$$Q_{bh} = -V \cdot \Delta \ln (C/C_0) / \Delta t$$

3-1

where Q_{bh} (m^3/s) is the groundwater flow rate through the borehole section and V is the volume of the borehole section (m^3).

Table 3-3 Tracers used in STT-1b, half-lives and maximum concentrations (activities) measured in the injection loop.

| Tracer | Half-life | Injection conc. C_0 * |
|--------------------------------|-----------|-------------------------|
| Uranine | - | 85.8 mg/l |
| HTO (Tritiated water) | 12.3 y | 293 000 Bq/g |
| ^{82}Br (Bromine) | 35.3 h | 4381.2 Bq/g |
| ^{131}I (Iodine) | 8 d | 2632.9 Bq/g |
| ^{22}Na (Sodium) | 2.6 y | 2657.7 Bq/g |
| ^{42}K (Potassium) | 12.4 h | 4373.1 Bq/g |
| ^{99m}Tc (Technetium) | 6.0 h | 8142.9 Bq/g |
| ^{86}Rb (Rubidium) | 18.7 d | 5248.9 Bq/g |
| ^{85}Sr (Strontium) | 64.9 d | 1254.7 Bq/g |
| ^{58}Co (Cobalt) | 71.3 d | 7545.2 Bq/g |

* maximum concentration measured in the injection loop.

In Figure 3-2 the injection concentrations for the different tracers are plotted in the same diagram versus time and normalised to the maximum injection concentration (activity), cf. Table 3-3. It clearly shows the effect of sorption on the borehole walls in the injection interval resulting in a much faster decrease in concentration for the more strongly sorbing species like Co and Rb. Thus, only the conservative tracers were used to determine injection flow rates. The dilution curve for the conservative tracer Uranine is shown in Figure 3-3. The calculated injection flow rates (compensated for sample volumes) are given in Table 3-4. The tracer injection curve for Uranine is also presented in log-log scale in Appendix.

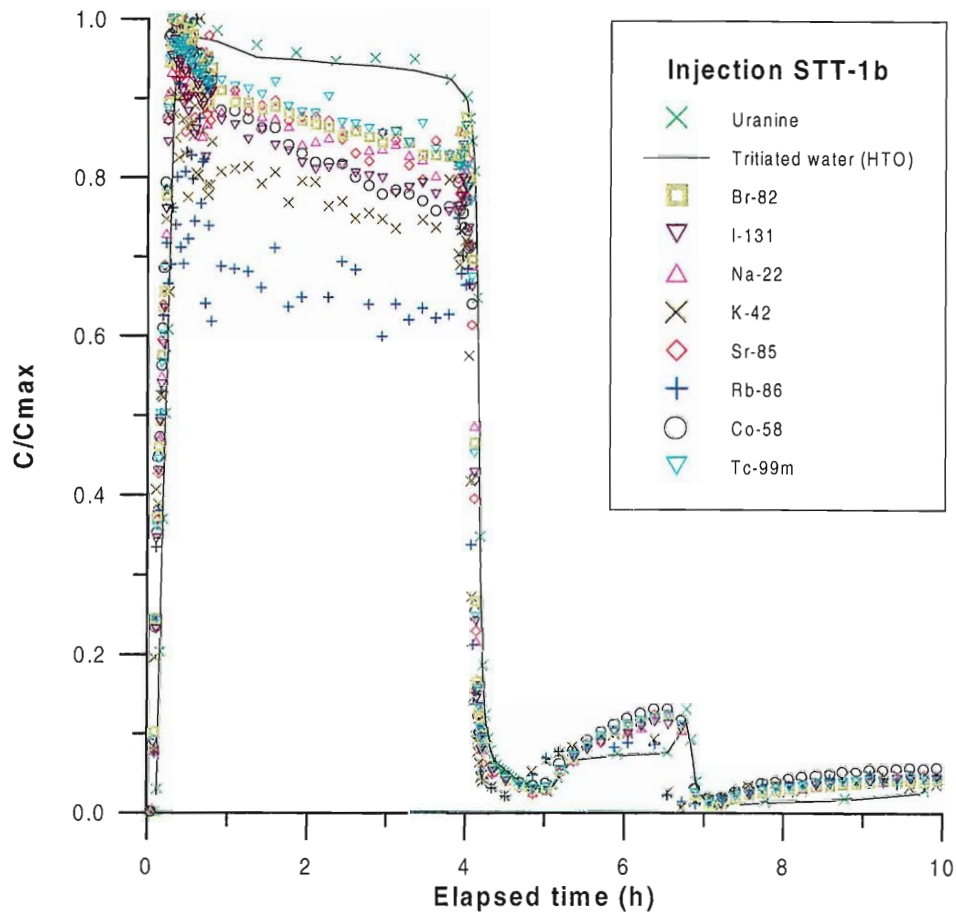


Figure 3-2. Tracer injection concentrations (activities) normalised to maximum measured concentration (activity) in the injection section KXTT1 R2 during the first 10 hours of injection.

The concentration of the conservative tracers Uranine and tritiated water (HTO) are higher and also somewhat delayed compared to the sorbing ones during the rising and falling parts of the curve. This is an effect of the different sampling/detection systems where the sorbing species are measured in-line and Uranine and HTO concentrations are derived from discrete samples resulting in samples averaged over a longer time period than in the in-line measurements. However, the delay is only about 5 minutes and is therefore not considered to be important for the evaluation of the test. The relative concentration is also higher due to the averaging of the maximum concentration. A similar effect can be seen between 5 and 10 hours of injection where the low sampling flow rate gives a significant delay for Uranine and HTO.

The time period between 4 and 10 hours requires some comments. After 4 hours of injection the tracer solution was exchanged with unlabelled water as described in Chapter 2.1.2. The exchange procedure lasted for one hour. Since the exchange procedure in STT-1 had not been so effective (Andersson et al., 1998) and the tracer concentration (activity) was increasing significantly in the injection section after the first exchange, a second exchange was made 6.7 hours after injection start. The second

exchange lasted for 25 minutes. The tracer exchange procedure gave a total reduction of about 95 % of the mass in the injection loop. The tracer solution was introduced into the borehole volume through a stainless steel tube perforated with several narrow holes to achieve optimal mixing at a certain pre-selected flow rate, in this case $q=10$ l/h. This system seems to be rather sensitive to variations in the flow rate such that a higher or lower flow rate may result in less mixing in parts of the borehole volume, i.e. more or less stagnant volumes. Hence, when the exchange procedure is finished, tracer labelled water from these more stagnant parts of the borehole volume slowly mixes with the remaining volume and the concentration of tracer rises again, cf. Figure 3-2 and 3-3.

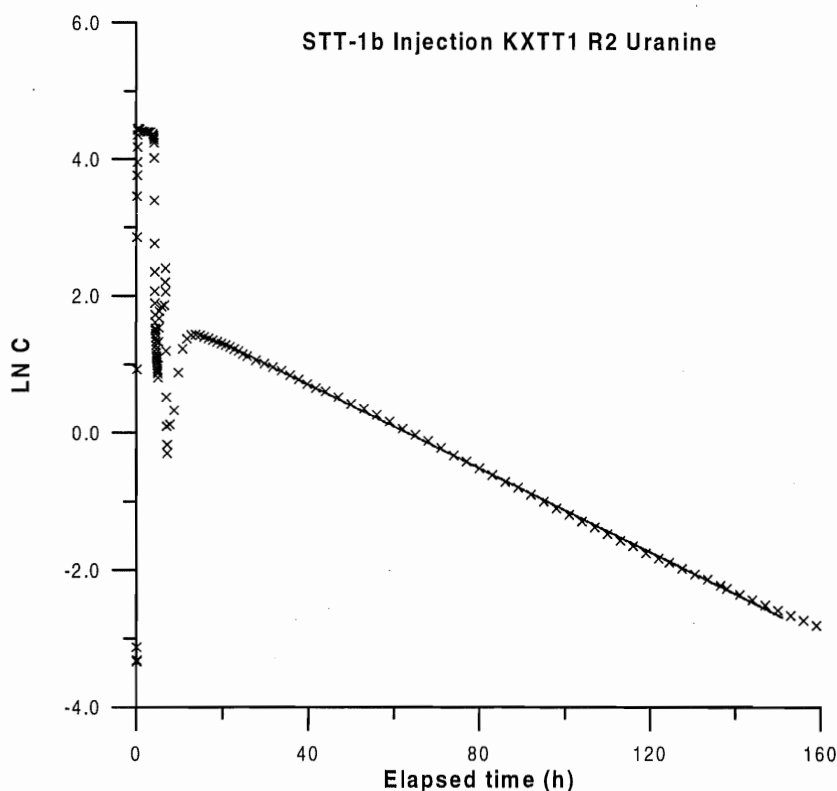


Figure 3-3. Tracer injection concentration ($\ln C$) versus elapsed time, t (h), for Uranine in the injection section KXTT1 R2 during the first 160 hours of injection in STT-1b. The straight line represents the least-square regression fit.

Two time periods with somewhat different injection flow rates were identified, cf. Table 3-4 and Figure 3-3. During the first period (0-4 h) the calculated flow rates for Uranine and tritiated water (HTO) are very consistent while they for ^{82}Br and ^{131}I are much higher. The time period after the exchange procedure shows more consistent flow rates for all four tracers. For all calculations of mass flux and recovery presented in this report, the values determined for Uranine have been used. Due to the few data points between 0-20 hours, the flow rate determined for the time period 20-151 hours was also used for the period 0-20 hours.

When evaluating tracer mass recovery by integration of the breakthrough data over time it was found that the calculated mass recoveries were consistently >100 %. This was also observed during PDT-3 (Andersson & Wass, 1998) and STT-1 (Andersson et al., 1998). The conclusion is that assigning a too small volume of the borehole section used in Equation 3-1 may cause the calculated excess mass recovery. Such an error may occur even if the borehole and dummy diameters are only a few tenths of a millimetre different from what have been assumed as nominal. Thus, by increasing the borehole volume in KXTT1 R2 from 1560 ml to 1999 ml (28 %) a recovery of 100 % was achieved.

Table 3-4 Injection flow rates at different time periods during STT-1b calculated from the dilution of the conservative tracers used. R is the correlation coefficient for the straight line fit.

| Tracer | Elapsed time (h) | Flow (ml/h) | R |
|---------|------------------|-------------|--------|
| Uranine | 0-4 | 41.9 | 0.9212 |
| | 20-151 | 58.1 | 0.9995 |
| HTO | 0-4 | 41.7 | 0.9142 |
| | 20-169 | 61.0 | 0.9997 |
| Br-82 | 0-4 | 72.1 | 0.9076 |
| | 10-130 | 53.4 | 0.9941 |
| I-131 | 0-4 | 81.3 | 0.9499 |
| | 28-115 | 51.6 | 0.9982 |

3.4 Tracer breakthrough

3.4.1 Tracer breakthrough data interpretation

Tracer breakthrough in the pumping section was monitored for nine of the ten tracers injected. The tracer not detected in the pumping section was ^{99m}Tc . The breakthrough curves (Figures 3-4 and 3-5) show one high and distinct single peak. Breakthrough data for ^{42}K were very scattered due to the large uncertainties in the activity data caused by

the short half-life of ^{42}K in combination with large analysis errors. Both figures show concentrations (activities) normalised to the injection concentration at $t=2$ hours in order to get a good comparison between the different species. The reason for not choosing the maximum concentration is that the value is more uncertain due to the concentration peak during the initial part of the injection. All nine breakthrough curves are presented in log-log scale in Appendix together with the breakthrough curve (log-log scale) for ^{137}Cs injected during STT-1 (Andersson et al., 1998).

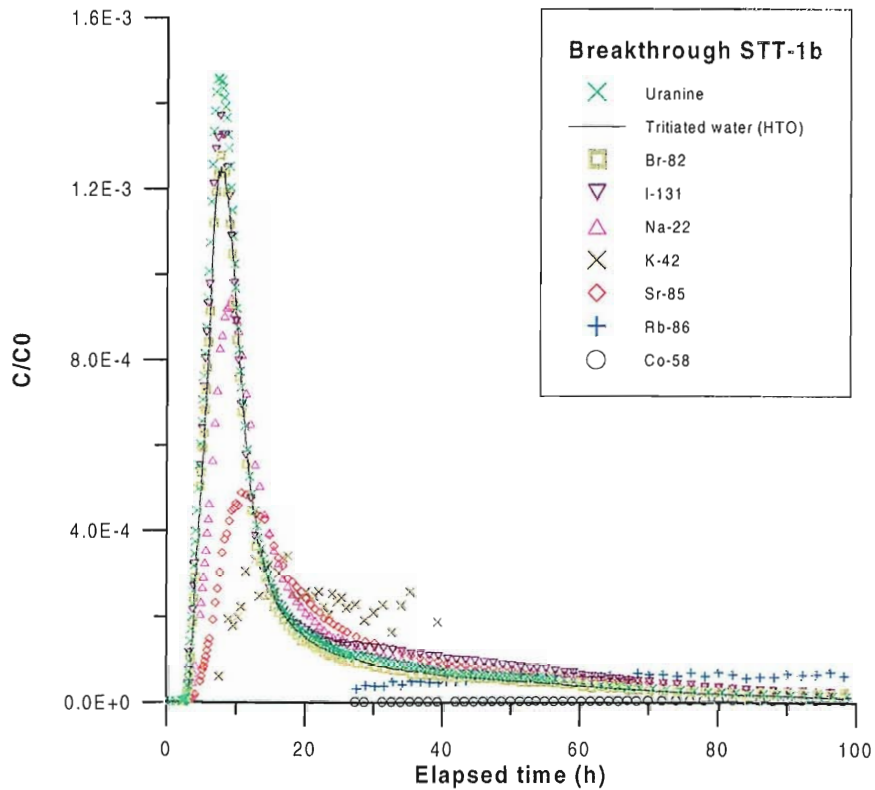


Figure 3-4. Tracer breakthrough after 100 hours in the pumping section KXTT3 R2 during STT-1b. Tracer concentrations are normalised to injection concentrations at $t=2$ hours.

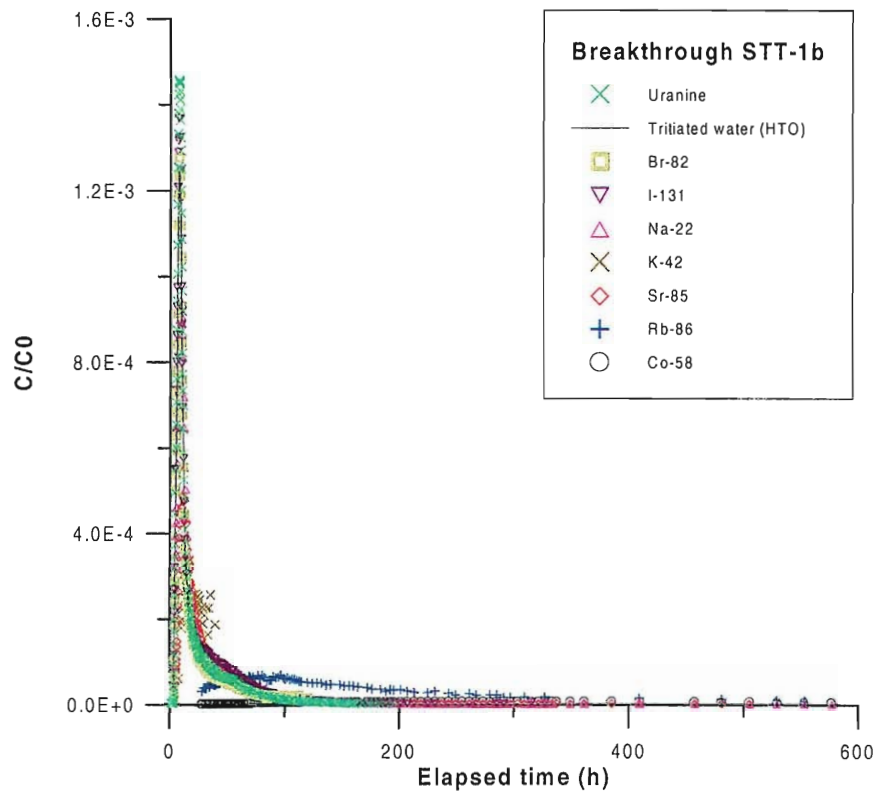


Figure 3-5. Tracer breakthrough after 580 hours in the pumping section KXTT3 R2 during STT-1b. Tracer concentrations are normalised to injection concentrations at $t=2$ hours.

Tracer travel times, t_5 , t_{50} and t_{95} , defined as times when 5, 50 and 95 % of the recovered mass has arrived in the pumping section, based on injected mass at t_{inj} , were calculated (Table 3-5). The time t_{inj} corresponds to the time at which the monitoring of the injection concentration is terminated.

Table 3-5 Tracer travel times, t_5 , t_{50} and t_{95} based on injected mass at t_{inj} for tracers injected during STT-1b.

| Tracer | t_5 (h) | t_{50} (h) | t_{95} (h) | t_{inj} (h) |
|---------|-----------|--------------|--------------|---------------|
| Uranine | 5.0 | 11 | 80 | 192 |
| HTO | 5.3 | 12 | - | 186 |
| Br-82 | 5.2 | 13 | - | 119 |
| I-131 | 5.3 | 17 | - | 320 |
| Na-22 | 6.5 | 17 | 900 | 164 |
| K-42 | 10 | 30 | - | 18 |
| Sr-85 | 8.3 | 35 | - | 248 |
| Rb-86 | 43 | 176 | - | 140 |
| Co-58 | 285 | - | - | 1980 |

Based on the mean travel times, t_m , determined from the parameter estimation of the conservative tracers (cf. Section 3.4.2), values the fracture conductivity, K_{fr} (m/s), were calculated for STT-1b assuming radial flow and validity of Darcy's law (Gustafsson & Klockars, 1981);

$$K_{fr} = \ln(r/r_w) \cdot (r^2 - r_w^2) / 2 \cdot t_m \cdot \Delta h \quad 3-2$$

where: r = travel distance (m)

r_w = borehole radius (m)

t_m = mean travel time of tracer (s)

Δh = head difference (m)

The equivalent fracture aperture, b (m), was calculated from:

$$b = Q \cdot t_m / \pi \cdot (r^2 - r_w^2) \quad 3-3$$

where Q (m^3/s), is the mean pumping rate.

Flow porosity, θ_k , was calculated using:

$$\theta_k = K/K_{fr} \quad 3-4$$

where K is the hydraulic conductivity of the packed-off section of the borehole determined from steady state evaluation of the interference test (Moye's formulae):

$$K = (Q/\Delta h \cdot L) \cdot ((1 + \ln L/2r_w)/2\pi) \quad 3-5$$

where L (m) is the length of the packed-off section. It should be noted that the term flow porosity might be misleading to use in a fractured heterogeneous rock as it is defined for a porous media. However, it is often used in fractured media as a scaling factor for transport, but then defined over a finite thickness which, in his case, is defined as the length of the packed-off borehole section ($L = 2.0$ m).

The values calculated using Equations 3-2 to 3-4 are presented together with parameters determined from the numerical modelling of the conservative tracer breakthrough in Table 3-6.

3.4.2 Numerical modelling

The breakthrough curves from STT-1b were evaluated using the one-dimensional advection-dispersion equation with linear sorption (for example Van Genuchten and Alves, 1982):

$$R \frac{\partial C}{\partial t} = -v \frac{\partial C}{\partial l} + D_1 \frac{\partial^2 C}{\partial^2} \quad 3-6$$

where

t is time (s), l is distance along flow path (m), v is the average water velocity along the flow path (m/s), C is the solute concentration, D is the dispersion coefficient (m^2/s), and R is the retardation coefficient.

The following initial and boundary conditions were used:

$$C(l,t) = 0 \quad t = 0 \quad 3-7$$

$$\frac{\partial C(l,t)}{\partial l} = 0 \quad l = \infty \quad 3-8$$

$$-D \frac{\partial C}{\partial l} + vC = vf(t) \quad l = 0 \quad 3-9$$

where the input function $f(t)$ is:

$$f(t) = C_0 \quad 0 < t \leq t_0 \quad 3-10$$

$$f(t) = 0 \quad t > t_0$$

where C_0 is the input concentration and t_0 is the time duration of the input period.

Variable tracer input concentration was simulated by superimposing solutions of the above equations. The measured input tracer concentrations were discretised into time intervals, where each time interval was assigned a constant input concentration.

The model was used to estimate parameters using an automated parameter estimation program, PAREST (Nordqvist, 1994). The program uses non-linear least square regression. This method finds the best-fit parameters by an iterative procedure, which is thoroughly described in Andersson et al. (1998).

One of the most interesting parameters to estimate in this case is the retardation factor for the various sorbing tracers. This was accomplished by applying two breakthrough curves simultaneously in the regression procedure. One of the tracers was then considered conservative, while the retardation factor for the other tracer relative to the first one could be determined.

The parameters that were estimated were the average velocity (v), dispersion coefficient (D), the retardation factor (R), and two proportionality factors (f and f_c). The factor f represents the dilution caused by the flow field, while the factor f_c simply is the injection concentration of the retarded tracer relative to the conservative one. Whether these factors are estimated or considered known (from measurements) is a subjective choice of the interpreter. In this case it was decided to estimate the proportionality factors, and check whether the values appeared to be reasonable when compared to independent measurements of pumping rates and input concentrations.

The perhaps more common approach to determine R is to estimate v from each breakthrough curve simultaneously, and then take the ratio of the velocities. However, the approach used here should give better results, because both curves are forced to have the same dispersion coefficient and dilution factor (f), which should help revealing model errors. In addition, estimation errors for the parameters should be lower because more points are used in the regression.

Another concern when using multiple data sets for regression is that magnitudes of the dependent variable may differ considerably. This is handled in this case by using the reliability weight matrix, \mathbf{W} . Each observation was assigned a weight reflecting the analytical uncertainty of the tracer sample. Standard deviations of the laboratory analyses of the nuclides were obtained based on the measurement time in the laboratory, while the Uranine measurements were assigned an error of one percent of a value down to the detection limit. All nuclide observations were assigned weights amounting to the inverse of the variance (standard deviation squared), while the weights for the Uranine samples were assumed to be the inverse of the assumed error.

The model simulations for STT-1b included two different runs for each tracer. First a separate run for each tracer assuming conservative transport (no retardation) where all transport processes are described as some apparent equivalent dispersivity. This run serves as a check of input data files and also produces a mean travel time for each tracer.

Secondly, each sorbing tracer breakthrough curve was fitted simultaneously with the conservative tracer Uranine.

The injection was simulated for each tracer by discretisation of the measured input function in 40-50 time steps. Figure 3-6 shows the discretisation of the first 25 hours of the input function for Uranine.

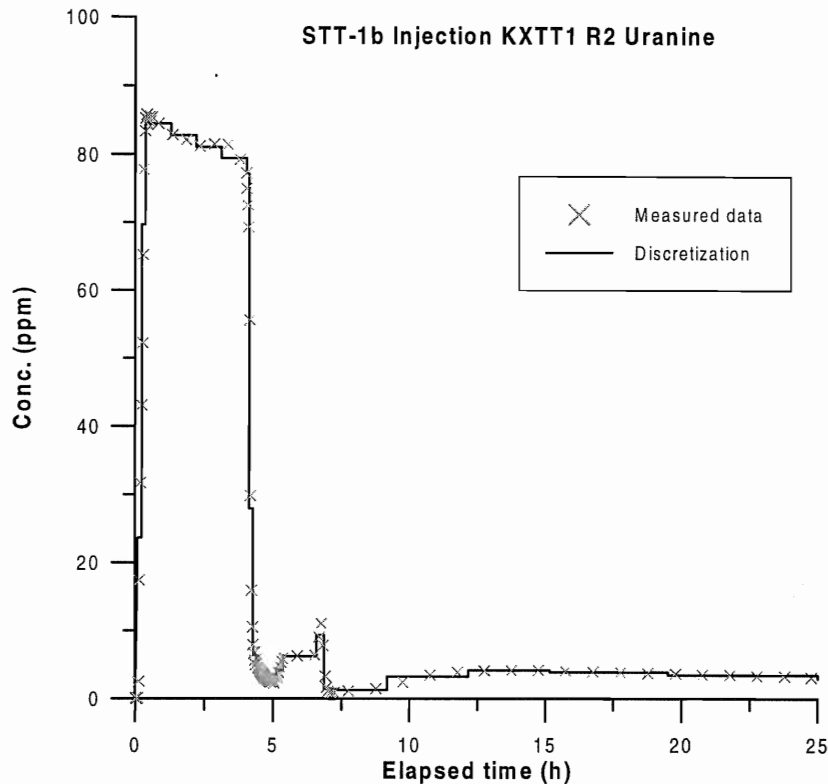


Figure 3-6. Discretisation of tracer injection function for Uranine in section KXTT1 R2 during STT-1b used for modelling using PAREST.

The best fit run for Uranine is shown in Figure 3-7 and the resulting parameters are given in Table 3-6 where also the values determined from STT-1 are shown. The regression statistics show low standard errors (1-2 %) and a relatively low correlation between parameters (indicating robust parameter estimates).

Table 3-6 Summary of measured and evaluated parameters for the flow path KXTT1 R2 → KXTT3 R2 from STT-1b and for the flow path KXTT4 R3 → KXTT3 R2 from STT-1.

| Parameter | STT-1b | STT-1 | Source |
|---|---------------------------|---------------------------|------------|
| | Value | Value | |
| Travel distance, L (m) | 5.03 | 4.68 | geometry |
| Mean head difference, Δh (m) | 9.5 | 7.2 | measured |
| Mean velocity, v (m/s) | $2.3 \cdot 10^{-4}$ (0.5) | $2.5 \cdot 10^{-4}$ (1.1) | PAREST |
| Mean travel time, t_m (hours) | 6.1 (0.5) | 5.1 (1.1) | PAREST |
| First arrival, t_a (hours) | 2.5 | 1.5 | measured |
| Dispersivity, D/v (m) | 0.55 (1.8) | 2.0 (2.8) | PAREST |
| Peclet Number, Pe | 9.1 | 2.3 | PAREST |
| Fracture conductivity, K_{fr} (m/s) | $3.1 \cdot 10^{-4}$ | $4.2 \cdot 10^{-4}$ | Eq. 3-2 |
| Equivalent fracture aperture, b (m) | $1.8 \cdot 10^{-3}$ | $1.8 \cdot 10^{-3}$ | Eq. 3-3 |
| Flow porosity (2 m thickness), θ_k | $1.1 \cdot 10^{-3}$ | $1.5 \cdot 10^{-3}$ | Eq. 3-4 |
| Mass recovery, R (%) | 100 | 100 | calculated |

The modelling of each tracer separately generally resulted in good fits for all tracers (Figure 3-8 and 3-9) with the exception of ^{42}K where the data set is very scattered and ^{85}Sr where the peak is underestimated. This is also reflected by the standard errors, which are between 1-6 % for all tracers except ^{42}K where the errors are between 11-16 %. However, the use of weights reduces the importance of data points with large errors and still makes it possible to get a reasonably good fit. The parameters determined from the model runs of separate tracers are presented in Table 3-7. It should be noted that the calculated dispersivity values include all processes in this case and should not be used as “true” values.

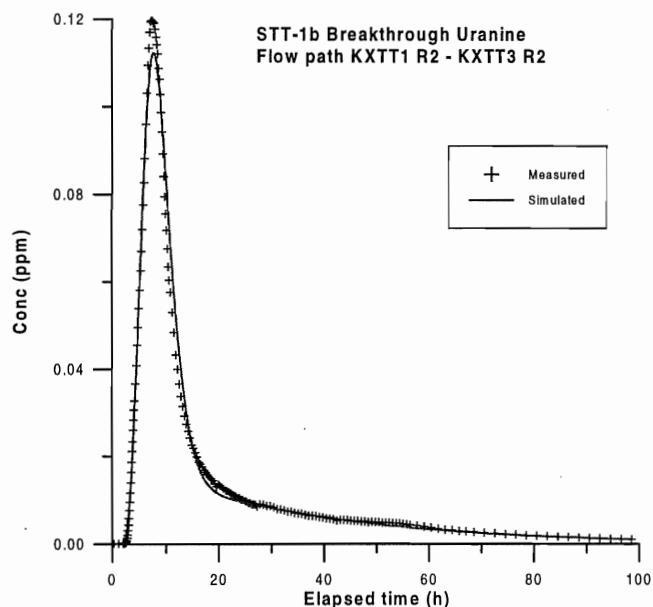


Figure 3-7. Comparison between measured and simulated breakthrough of Uranine in the pumping section KXTT3 R2 during STT-1b.

Table 3-7 Evaluated parameters from STT-1b using PAREST (advection-dispersion model). Separate runs for each tracer. Values within brackets are standard errors in percent.

| Tracer | Mean velocity, v (m/s) | Mean travel time, t_0 (h) | Dispersivity*, D/v (m) | Proportionality factor, F |
|---------|-----------------------------|--------------------------------|-----------------------------|--------------------------------|
| Uranine | $2.3 \cdot 10^{-4}$ (1) | 6.1 (1) | 0.55 (2) | $2.4 \cdot 10^{-3}$ (1) |
| HTO | $2.1 \cdot 10^{-4}$ (1) | 6.6 (1) | 0.46 (2) | $2.3 \cdot 10^{-3}$ (1) |
| Br-82 | $2.3 \cdot 10^{-4}$ (1) | 6.1 (1) | 0.43 (4) | $2.0 \cdot 10^{-3}$ (2) |
| I-131 | $2.3 \cdot 10^{-4}$ (1) | 6.1 (1) | 0.45 (3) | $2.2 \cdot 10^{-3}$ (2) |
| Na-22 | $1.6 \cdot 10^{-4}$ (1) | 8.6 (1) | 0.69 (5) | $2.2 \cdot 10^{-3}$ (2) |
| K-42 | $6.0 \cdot 10^{-5}$ (11) | 23.3 (11) | 2.0 (16) | $2.3 \cdot 10^{-3}$ (13) |
| Sr-85 | $9.4 \cdot 10^{-5}$ (3) | 14.9 (3) | 1.9 (6) | $1.7 \cdot 10^{-3}$ (2) |
| Rb-86 | $1.1 \cdot 10^{-5}$ (2) | 123 (2) | 3.9 (4) | $2.1 \cdot 10^{-3}$ (2) |
| Co-58 | $2.1 \cdot 10^{-6}$ (2) | 672 (2) | 6.2 (2) | $1.1 \cdot 10^{-3}$ (2) |

* Include all possible forms of heterogeneity and retention processes.

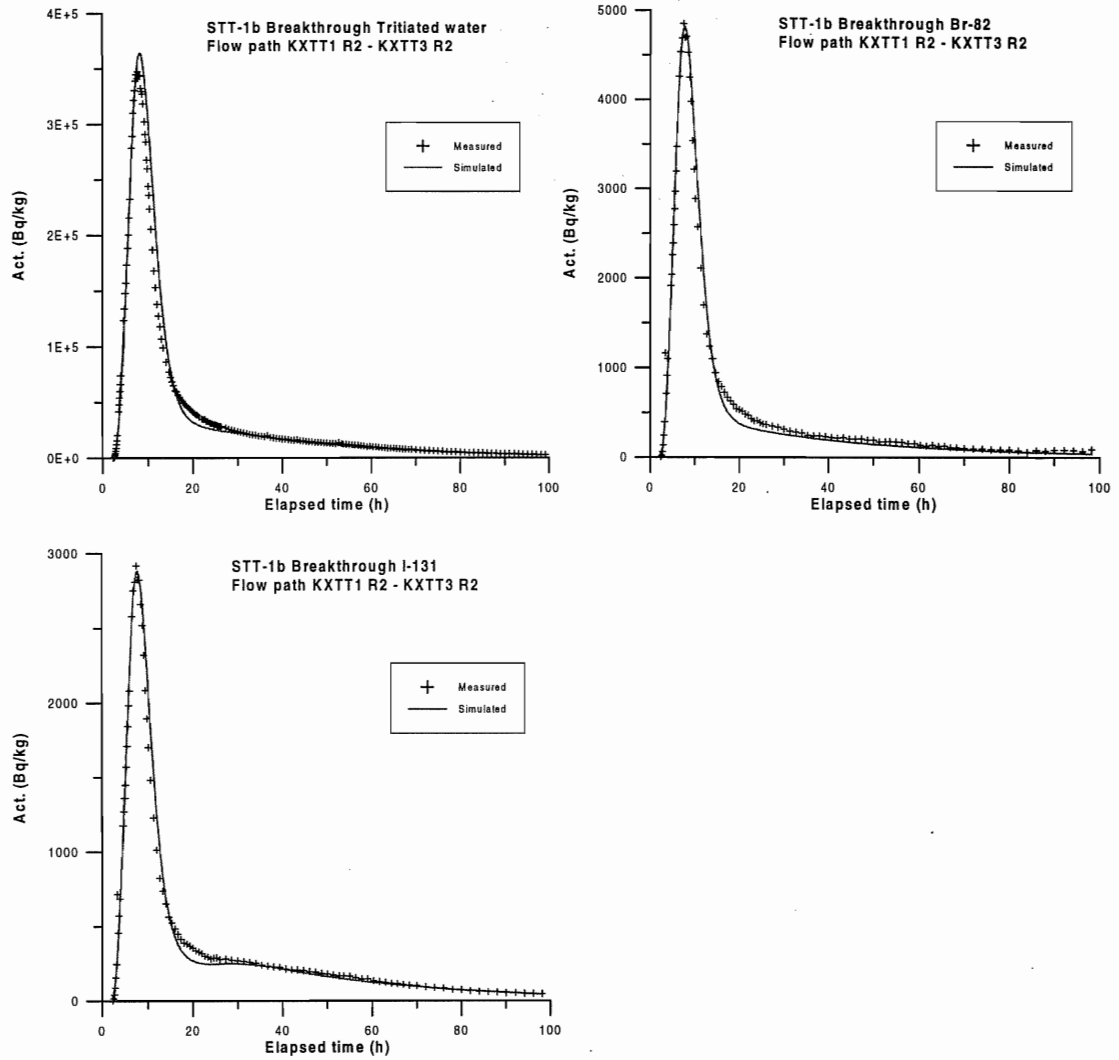


Figure 3-8. Comparison between measured and simulated breakthrough of the radioactive (conservative) tracers in the pumping section KXTT3 R2 during STT-1b. Separate runs for each tracer, a) Tritiated water (HTO), b) Br-82, c) I-131.

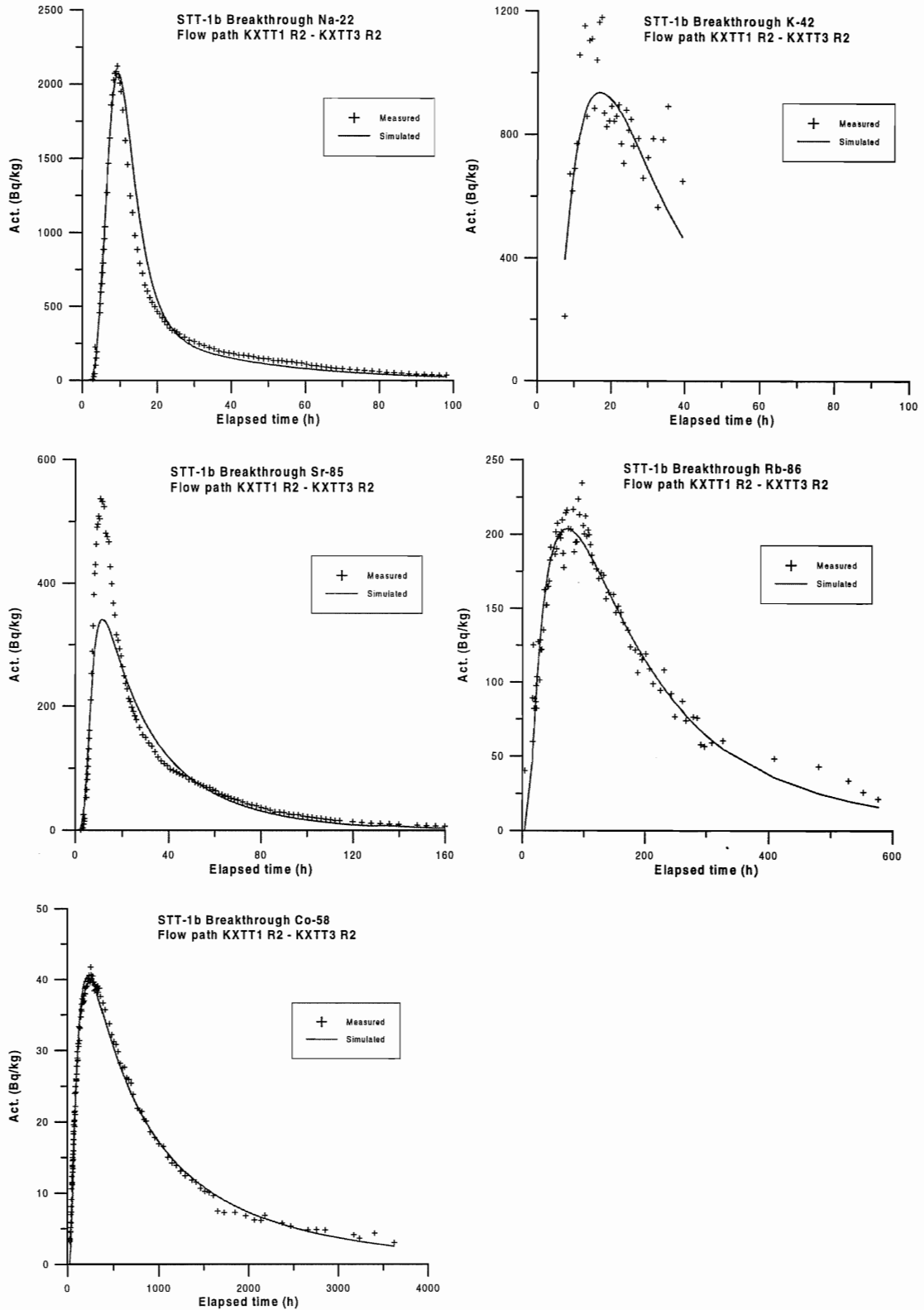


Figure 3-9. Comparison between measured and simulated breakthrough of the radioactive (sorbing) tracers in the pumping section KXTT3 R2 during STT-1b. Separate runs for each tracer, a) Na-22, b) K-42, c) Sr-85, d) Rb-86, e) Co-58.

The model runs using simultaneous fit of the conservative tracer Uranine and a sorbing tracer are presented in Figure 3-10 and the parameter values are given in Table 3-8. The values of mean travel time, dispersivity and proportionality factor are in general quite consistent with low standard errors, 1-4 %. Retardation coefficients vary between 1.4 for ^{22}Na up to 57 for ^{58}Co .

The respective fits to the experimental data are in general not as good as for individual runs with this simple model, as expected. The model can fit the breakthrough curves for ^{22}Na and ^{85}Sr relatively well while the fits for ^{86}Rb and ^{58}Co are much worse especially in the tail part, cf. Figure 3-9. This indicates that the retardation of ^{86}Rb and ^{58}Co cannot be explained by a simple surface sorption model alone. The values for ^{42}K are more uncertain due to the uncertainties in the data.

Table 3-8 Evaluated parameters for STT-1b using PAREST (advection-dispersion-linear sorption model). Simultaneous runs with Uranine and a sorbing tracer. Values within brackets are standard errors in percent.

| Tracer | v (m/s) $\cdot(10^{-4})$ | t_0 (h) | D/v (m) | $F \cdot(10^{-3})$ | R | f_c |
|---------|----------------------------|-----------|-----------|--------------------|-----------|----------|
| Uranine | 2.29 (1) | 6.1 (1) | 0.55 (2) | 2.4 (1) | 1 | 1 |
| Na-22 | 2.26 (1) | 6.2 (1) | 0.59 (2) | 2.4 (1) | 1.37 (1) | 0.95 (2) |
| K-42 | 2.29 (1) | 6.1 (1) | 0.55 (2) | 2.4 (1) | 2.77 (15) | 555 (17) |
| Sr-85 | 2.26 (1) | 6.2 (1) | 0.60 (2) | 2.4 (1) | 1.86 (2) | 0.78 (3) |
| Rb-86 | 2.28 (1) | 6.1 (1) | 0.56 (2) | 2.4 (1) | 17.0 (5) | 0.49 (6) |
| Co-58 | 2.16 (1) | 6.5 (1) | 0.80 (4) | 2.2 (2) | 57.0 (2) | 0.21 (5) |

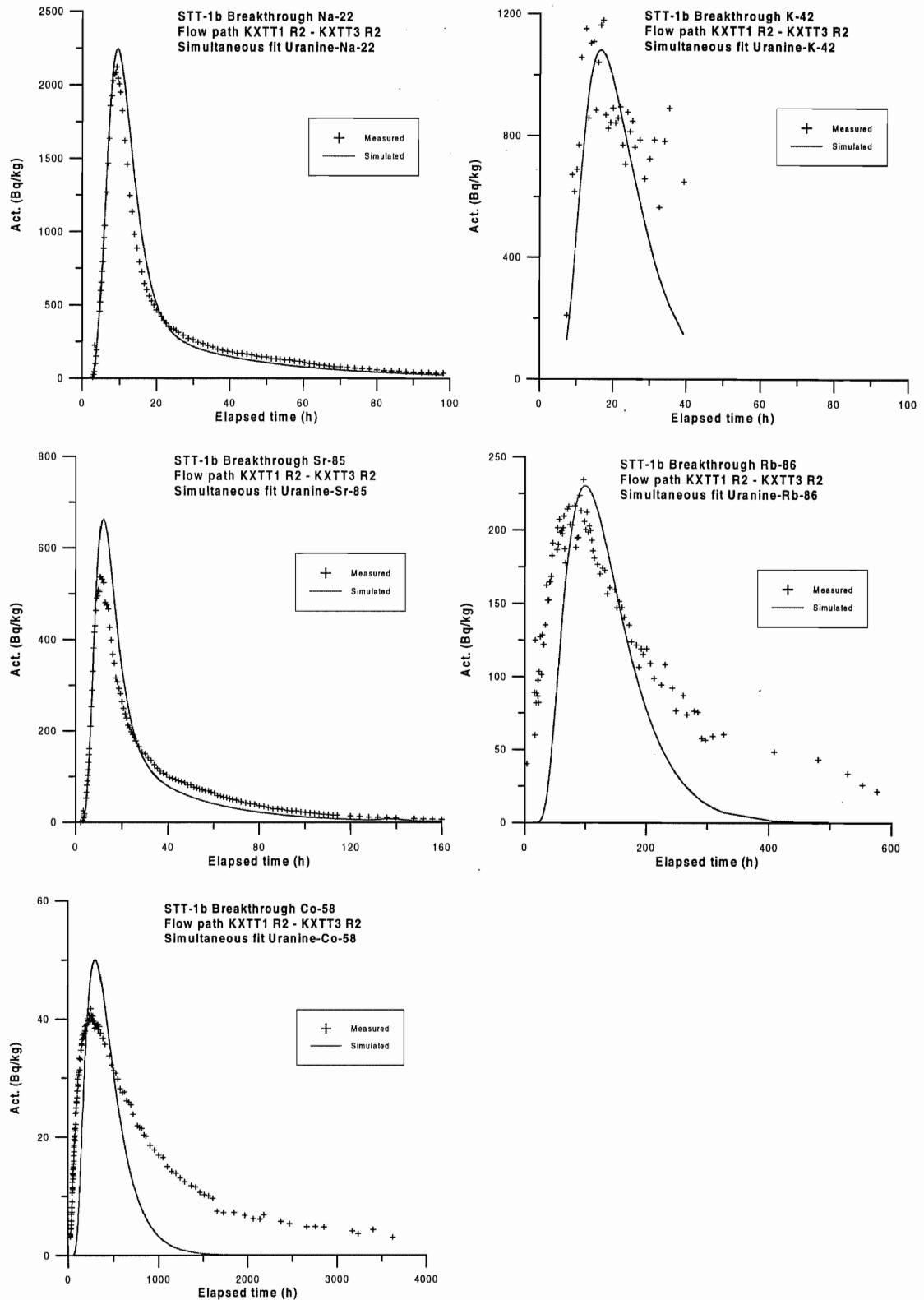


Figure 3-10. Comparison between measured and simulated breakthrough of the radioactive (sorbing) tracers in the pumping section KXTT3 R2 during STT-1b. Simultaneous run of Uranine and, a) Na-22, b) K-42, c) Sr-85, d) Rb-86, e) Co-58.

3.4.3 Tracer mass recovery

Tracer mass recovery was calculated in two different ways for the nine tracers detected in the pumping section. Common for both methods was that the tracer mass recovered in the pumping borehole was determined by integration of the breakthrough curves for mass flux (mg/h or Bq/h) versus time (h). The injected mass was determined in the same way but also by weighing and measuring the concentration of the tracer solution removed from the injection section during the exchange procedure and calculating the difference with the known mass added to the stock solution (mass balance), cf. Table 3-9.

The mass recovery calculated from integration is in general higher (except for Uranine) than the measured ones and the difference is rather large. The reason for this may be that the injected mass was only a small portion of the total mass in the stock solution. Hence, a relatively large uncertainty can be expected in the determination of injected mass from weighing. Based on these considerations the mass recovery values determined from integration of the injection and breakthrough curves are considered to be the most appropriate to use.

Table 3-9 Tracer mass recovery during STT-1b determined by integration, R_i , and by weighing, R_w (t_t is the time for the last sample taken).

| Tracer | R_i (%) | R_w (%) | T_t (h) |
|---------|-----------|-----------|-----------|
| Uranine | 100 | 156 | 195 |
| HTO | 94 | 79 | 333 |
| Br-82 | 90 | 57 | 120 |
| I-131 | 90 | 60 | 327 |
| Na-22 | 96 | 58 | 1292 |
| K-42 | 70 | 24 | 39 |
| Sr-85 | 81 | 55 | 505 |
| Rb-86 | 93 | 58 | 553 |
| Co-58 | 29 | 18 | 3622 |

3.4.4 Cs-137 from STT-1

In the previous tracer test with sorbing tracers, STT-1 (Andersson et al., 1998), ^{137}Cs was injected on July 15th, 1997, in the flow path KXTT4 R3 → KXTT3 R2. The recovered mass of ^{137}Cs was only 26 % at the end of the test period on November 30th, 1997. It was therefore decided to follow the tailing of the breakthrough curve of ^{137}Cs during STT-1b until May 1998. The recovery at $t_t=7005$ h (t_t is the time for the last sample taken) was 33 %. The breakthrough curve is presented in log-log scale in Appendix A.

Model runs, both a separate run for ^{137}Cs and a simultaneous run of Uranine and ^{137}Cs (Figure 3-11), were made using the breakthrough data for the longer time period. The fit to the experimental ^{137}Cs data is also better in the separate run than in the simultaneous run, as for the tracers used in STT-1b, cf. Chapter 3.4.2. However, the separate run does not give any meaningful results other than for comparison with previous runs. The poor fit with the simultaneous run indicates that the retardation of ^{137}Cs cannot be explained with a simple surface sorption model.

The new model parameters are presented in Table 3-10 (separate run) and Table 3-11 (simultaneous run) together with the earlier determined values (Andersson et al., 1998). It can be seen that the values of mean travel time, dispersivity and retardation coefficient are higher using the extended breakthrough data set. The standard errors are quite low, 1-5 %, for both separate and simultaneous run, but are in general somewhat higher than the previous ones.

Table 3-10 Evaluated parameters for Cs-137 from STT-1 (flow path KXTT4 R3 → KXTT3 R2) using PAREST (advection-dispersion model), separate run. Comparison between parameters for $t_t=7005$ h and $t_t=1350$ h (t_t =time for last sample taken). Values within brackets are standard errors in percent.

| Parameter | $t_t=7005$ h | $t_t=1350$ h |
|-------------------------------|-------------------------|-------------------------|
| Mean velocity, v , (m/s) | $2.0 \cdot 10^{-6}$ (2) | $3.1 \cdot 10^{-6}$ (1) |
| Mean travel time, t_0 , (h) | 651 (2) | 421 (1) |
| Dispersivity, D/v , (m) | 18.6 (4) | 7.3 (3) |
| Proportionality factor, F | $0.5 \cdot 10^{-3}$ (1) | $0.3 \cdot 10^{-3}$ (1) |

Table 3-11 Evaluated parameters for Cs-137 from STT-1 (flow path KXTT4 R3 → KXTT3 R2) using PAREST (advection-dispersion-linear sorption model). Simultaneous run of Uranine and Cs-137. Comparison between parameters for $t_t=7005$ h and $t_t=1350$ h (t_t =time for last sample taken). Values within brackets are standard errors in percent.

| Parameter | $t_t=7005$ h | $t_t=1350$ h |
|-------------------------------|-------------------------|-------------------------|
| Mean velocity, v , (m/s) | $2.1 \cdot 10^{-4}$ (3) | $2.4 \cdot 10^{-4}$ (1) |
| Mean travel time, t_0 , (h) | 6.3 (3) | 5.3 (1) |
| Dispersivity, D/v , (m) | 6.3 (5) | 2.4 (3) |
| Proportionality factor, F | $1.7 \cdot 10^{-3}$ (2) | $1.7 \cdot 10^{-3}$ (1) |
| Retardation coefficient, R | 118.1 (4) | 69.4 (3) |
| f_c | 0.25 (2) | 0.13 (2) |

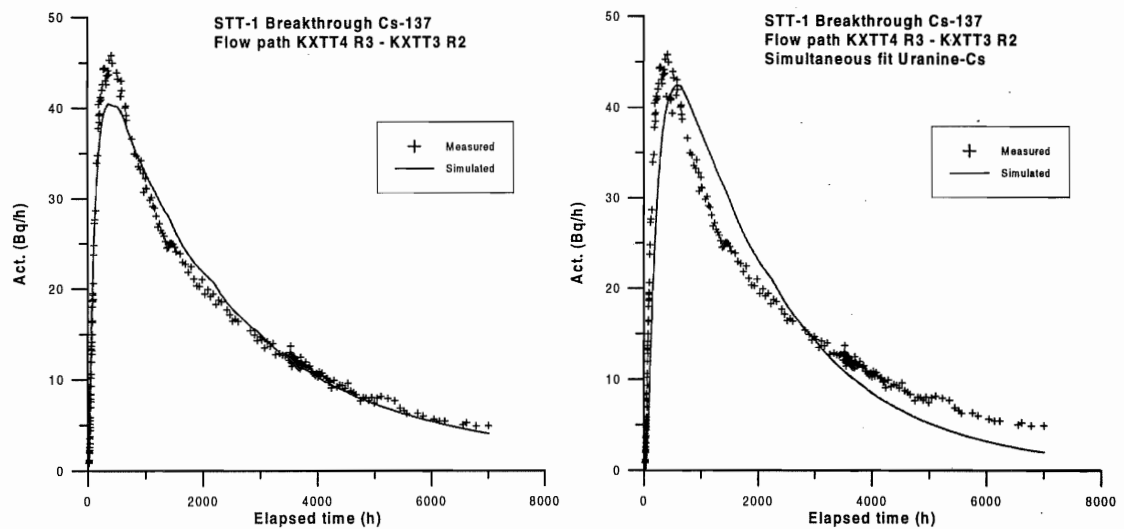


Figure 3-11. Comparison between measured and simulated breakthrough of Cs-137 in the pumping section KXTT3 R2 during STT-1. a) separate run, b) simultaneous run with Uranine.

3.5 Supporting data

The head distribution during the test period was governed by the imposed pumping in KXTT3 R2. The pumping rate in the withdrawal borehole section was stable and constant during the entire test, 0.401 l/min (Figure 3-12). The overall head variations during the period, illustrated by borehole HA1960A (Figure 3-13), which is a borehole penetrating the major bounding fracture zone NNW-4, are relatively large (± 2.5 m). The most prominent event is an increase in hydraulic head of about 3 m starting on January 19th caused by unknown reasons. The values of hydraulic head in Feature A presented in Figure 3-14 show similar variations as observed in HA1960A.

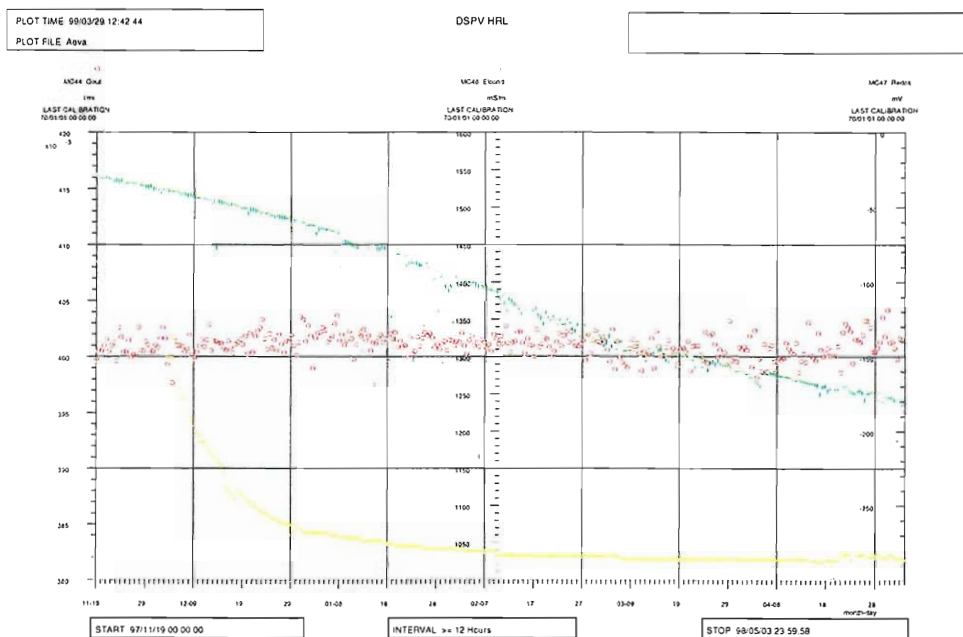


Figure 3-12. Pumping rate, electrical conductivity and redox potential of the pumped water in KXTT3 R2 during PDT-4 and STT-1b, November 19th, 1997 to May 3rd, 1998.

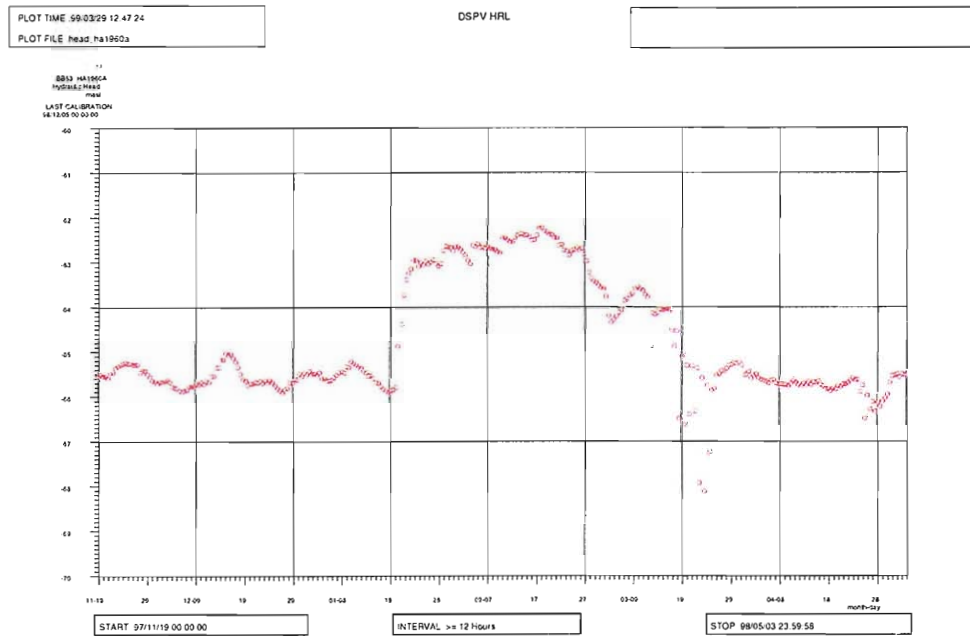


Figure 3-13. Hydraulic head in borehole HA1960A during PDT-4 and STT-1b, November 19th, 1997 to May 3rd, 1998.

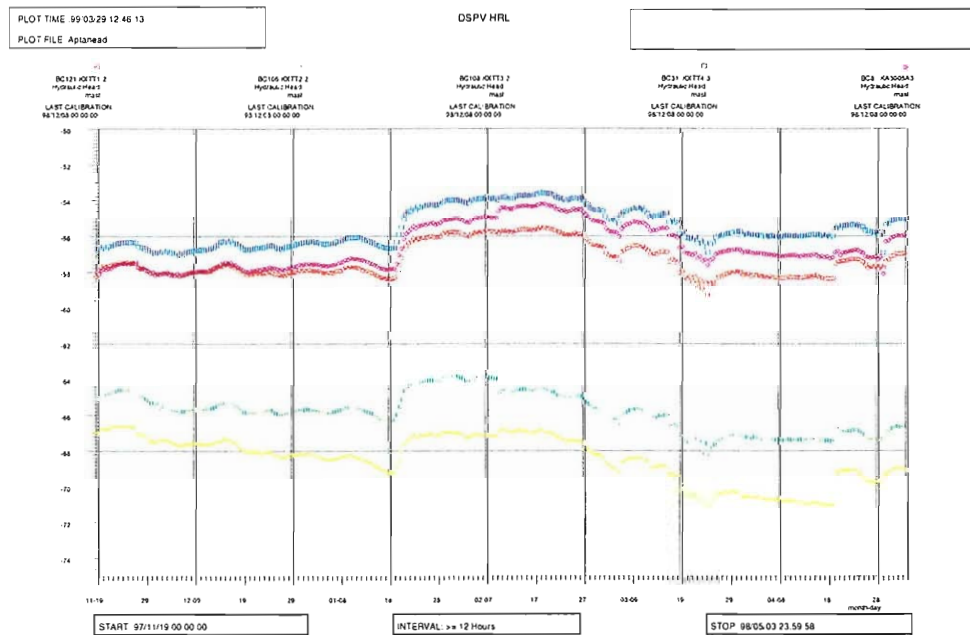


Figure 3-14. Hydraulic head in Feature A during PDT-4 and STT-1b, November 19th, 1997 to May 3rd, 1998.

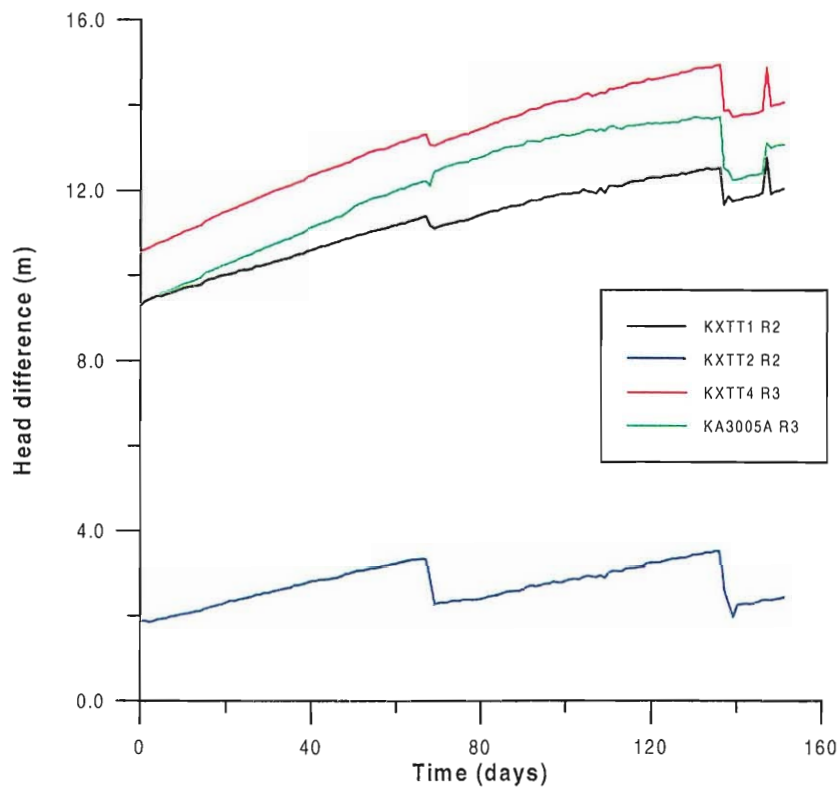


Figure 3-15. Head difference (m) versus time (days) for injection and observation sections compared to the pumping section KXTT3 R2 during STT-1b.

Figure 3-15 shows that the head difference to the pumping section KXTT3 R2 increases with time. This was also observed during STT-1. This could either be an effect of changes in hydraulic boundaries or that the local transmissivity in the pumping section decreases. The latter may result from chemical clogging effects caused by the pressure drop in the fracture close to the borehole.

4 Discussion and conclusions

4.1 Experimental set-up and performance

The experimental set-up for STT-1b was, with some modifications, identical to the one used in STT-1 (Andersson et al., 1998) and in PDT-3 (Andersson & Wass, 1998). The tracer exchange (ending of tracer pulse) during STT-1 was not very efficient, therefore the exchange procedure was repeated twice during STT-1b. The removal of tracer solution gave a reduction of about 95 % of the mass in the injection section which also resulted in a well defined and smooth breakthrough curve.

Plotting the injection and breakthrough curves (as mass flux versus time) in the same plot shows that the slow release of the 5% remaining tracer solution in the injection interval dominates the latter part of the breakthrough curve. This tailing may potentially mask important transport processes such as matrix diffusion or diffusion into stagnant parts of the flow path (Heer, pers. comm., 1999). Therefore, it is essential to reduce the initial tracer concentration at least down to 0.5% in future experiments. This will require a totally new instrument concept for the down-hole equipment as the current concept not was designed for finite pulse injections.

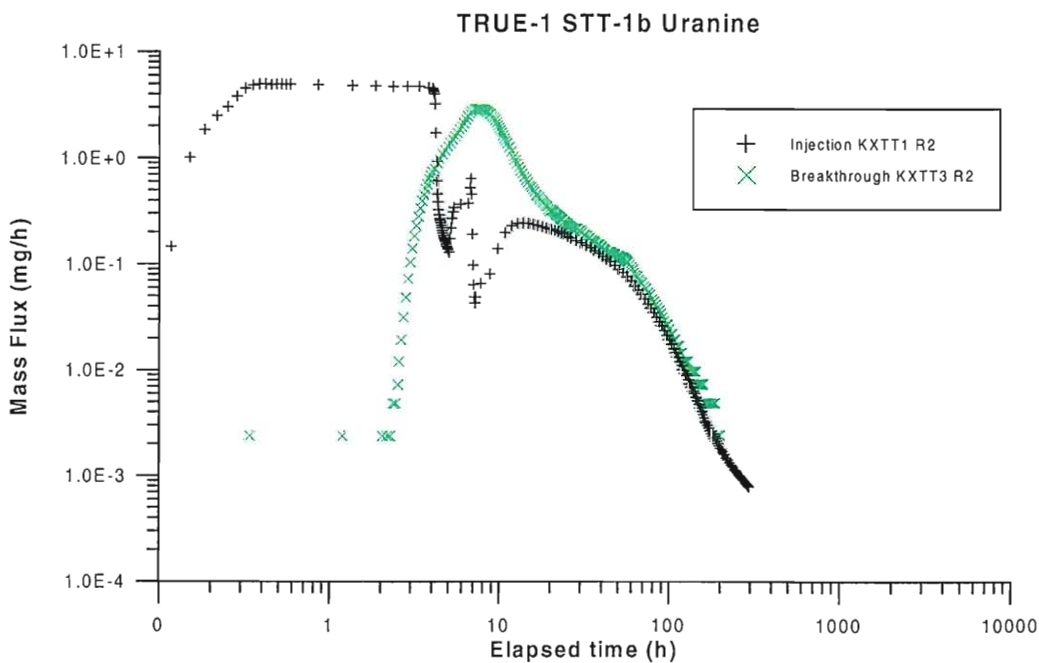


Figure 4-1. Tracer injection and breakthrough data (log-log scale) for Uranine from STT-1b, flow path KXTT1 R2 → KXTT3 R2.

A redox probe was also installed in the sampling loop for the withdrawn water due to the use of the redox-sensitive tracer Tc. The conclusion from STT-1 and PDT-3 that the system worked very well is also valid for STT-1b.

The injection procedure, during which the highest doses of radioactivity could be expected, was performed with very low doses to the personnel. The activity of the water discharged into the tunnel only showed a temporary increase of the background activity during the breakthrough.

The evaluation of tracer mass recovery showed some inconsistencies. Calculated mass recoveries based on integrated mass fluxes were found to be more than 100 % and differ considerably to values calculated based on weighing and concentration measurements of tracer mass from the exchange procedure. Based on earlier tests and uncertainties in the weighing and concentration measurements, the values determined by integration of the injection and breakthrough curves, corrected by assigning a larger (28 %) volume to the injection section, were considered to be the most appropriate to use, cf. Section 3.2.

4.2 Flow and transport in Feature A

The flow path KXTT1 R2 → KXTT3 R2 has earlier been tested in several different experiments. Table 4-1 summarises the flow and transport parameters derived from evaluation of seven different tests including PDT-4 and STT-1b. The values determined from STT-1b are similar to those determined from PTT-1 (Winberg *et al.*, 1996) and RC-1 (Andersson, 1996) that are the most appropriate values to compare with although the pumping rates were different. The remaining three tests (DP-1, PDT-1 and PDT-2) were performed with lower pumping rates, giving less mass recovery and somewhat deviating parameter values.

Table 4-1. Summary of flow and transport parameters determined for the flow path KXTT1 R2 → KXTT3 R2 (distance 5.03 m).

| Test | Q (l/min) | Δh (m) | R (%) | D/v (m) | K_{fr} (m/s) | b (m) | θ_k |
|--------|-------------|----------------|---------|-----------|---------------------|---------------------|---------------------|
| PTT-1 | 0.87 | 24 | 95 | (0.6)** | $3.5 \cdot 10^{-4}$ | $1.4 \cdot 10^{-3}$ | $1.0 \cdot 10^{-3}$ |
| RC-1 | 0.2 (0.4)* | 2.5 (5.6)** | 93 | 0.24 | $5.0 \cdot 10^{-4}$ | $2.2 \cdot 10^{-3}$ | $0.7 \cdot 10^{-3}$ |
| DP-1 | 0.1 | 5.8 | 88 | 0.40 | $2.8 \cdot 10^{-4}$ | - | $1.2 \cdot 10^{-3}$ |
| PDT-1 | 0.1 | 0.6 | 44 | 1.3 | $11 \cdot 10^{-4}$ | $2.1 \cdot 10^{-3}$ | $0.4 \cdot 10^{-3}$ |
| PDT-2 | 0.2 | 1.9 | 52 | 1.0 | $5.6 \cdot 10^{-4}$ | $2.6 \cdot 10^{-3}$ | $0.7 \cdot 10^{-3}$ |
| PDT-4 | 0.4 | 9.3 | 100 | - | - | - | - |
| STT-1b | 0.4 | 9.3-12.8 | 100 | 0.55 | $1.8 \cdot 10^{-4}$ | $1.8 \cdot 10^{-3}$ | $1.1 \cdot 10^{-3}$ |

* Pumping increased during experiment

** Uncertain due to transport in equipment

A comparison of the flow rate in the injection section KXTT1 R2 during RC-1 and STT-1b shows a significant increase from 44 to 58 ml/h (compensated for the increased volume in the section). This is also consistent with the observations from STT-1 for the injection interval KXTT4 R3 (Andersson et al., 1998). The measured flow is about a factor 10 higher than the background flow (5 ml/h) measured in April 1997 (Andersson & Wass, 1997) and represents a contribution corresponding to three borehole diameters, which is not far from the theoretical homogeneous porous case of two borehole diameters.

The increasing flow rate in the injection section and the increasing head difference between pumping and injection sections indicate a non-stationary flow field. The reason for these changes may be effects of hydraulic boundaries during this long-term pumping (8 months). Another explanation may be changes in the local transmissivity around the sections caused by chemical clogging, bacterial growth, etc.

The transport of the radioactive sorbing tracers showed significant retardation for all tracers. The retardation coefficients determined from a simple linear surface sorption model were found to vary between $R=1.4$ for ^{22}Na to $R=57$ for ^{58}Co . A comparison with retardation coefficients determined from laboratory data (Andersson et al., 1997a) and from STT-1 shows the same relative order and magnitude between the different species, whereas the parameter values from STT-1 and STT-1b are higher for all species (Table 4-2). The difference between STT-1 and STT-1b is small.

Table 4-2. Comparison between retardation coefficients, R , determined from laboratory data and from evaluation of STT-1.

| Tracer | R (lab)* | R (STT-1) | R (STT-1b) |
|--------|------------|-----------|------------|
| Na | 1.001-1.01 | 1.5 | 1.4 |
| Ca | 1.006-1.06 | 1.6 | - |
| Sr | 1.008-1.04 | 2.1 | 1.9 |
| K | - | - | 2.8 |
| Ba | 1.08-2.2 | 8.6 | - |
| Rb | 1.12-3.0 | 15 | 17 |
| Co | - | - | 57 |
| Cs | 2-21 | 69 | 118 |

* Determined from the equation $R=1+(2/b) \cdot K_a$, ($b=0.001$ m), where K_a (m) is the surface sorption coefficient determined in laboratory tests (Andersson et al., 1997a).

The applied simple model worked reasonably well in the simultaneous fit of the conservative tracer breakthrough (Uranine) and one of the weakly sorbing tracers ^{22}Na or ^{85}Sr . However, the fits using Uranine and the moderately sorbing tracers Rb and Co, individually, were not good, especially in the tail part of the breakthrough curves. Thus, the linear surface sorption process alone cannot explain the retardation of these species.

The tailing of the breakthrough curve for ^{137}Cs from the injection in the previous sorbing tracer test STT-1 was followed also during STT-1b. The recovered mass for ^{137}Cs at the end of the extended test period was 33 %. Model runs was made using breakthrough data for the longer test period and the new model parameters differ somewhat from the previous ones reported in Andersson et al. (1998). Values of mean travel time, dispersivity and retardation coefficient are higher using the extended breakthrough data set.

5 References

Andersson P, 1996: TRUE 1st stage tracer test programme. Experimental data and preliminary evaluation of the TRUE-1 radially converging tracer test (RC-1). Äspö Hard Rock Laboratory Progress Report HRL-96-24.

Andersson P, Jönsson S, 1997: TRUE 1st stage tracer test programme. Complementary Tracer Tests (RC-2, DP-5, DP-6). Experimental description and preliminary evaluation. Äspö Hard Rock Laboratory Progress Report HRL-97-23.

Andersson P, Wass E, 1997: TRUE 1st stage tracer test programme. Dilution tests, run # 2 March-April 1997. Äspö Hard Rock Laboratory Technical Note TN-97-26t.

Andersson P, Byegård J, Cvetkovic V, Johansson H, Nordqvist R, Selroos J-O, Winberg A, 1997a: TRUE 1st stage tracer test programme. Experimental plan for tests with sorbing tracers at the TRUE-1 site. Äspö Hard Rock Laboratory Progress Report HRL-97-07.

Andersson P, Nordqvist R, Jönsson S, 1997b: TRUE 1st stage tracer test programme. Experimental data and preliminary evaluation of the TRUE-1 dipole tracer tests DP-1 - DP-4. Äspö Hard Rock Laboratory Progress Report HRL-97-13.

Andersson P, Wass E, 1998: TRUE 1st stage tracer test programme. Preliminary Design Tests for tests with radioactive sorbing tracers (PDT-1, PDT-2, PDT-3). Experimental description and preliminary evaluation. Äspö Hard Rock Laboratory Progress Report HRL-98-13.

Andersson P, Johansson H, Nordqvist R, Skarnemark G, Skålberg M, Wass E, 1998: TRUE 1st stage tracer test programme. Tracer tests with sorbing tracers STT-1. Experimental description and preliminary evaluation. Äspö Hard Rock Laboratory Technical Note TN-98-10t.

Gustafsson E, Klockars C-E, 1981. Studies of groundwater transport in fractured crystalline rock under controlled conditions using non-radioactive tracers. Swedish Nuclear Fuel and Waste Management Company. SKBF/KBS Technical Report TR 81-07.

Heer W, 1999. Personal communication, January 1999.

Ittner T, Byegård J, 1997. First TRUE Stage. Test of tracer sorption on equipment. Äspö Hard Rock Laboratory Progress Report HRL-97-28.

Nordqvist R, 1994. Documentation of some analytical flow and transport models implemented for use with PAREST - Users manual. GEOSIGMA GRAP 94 006, Uppsala.

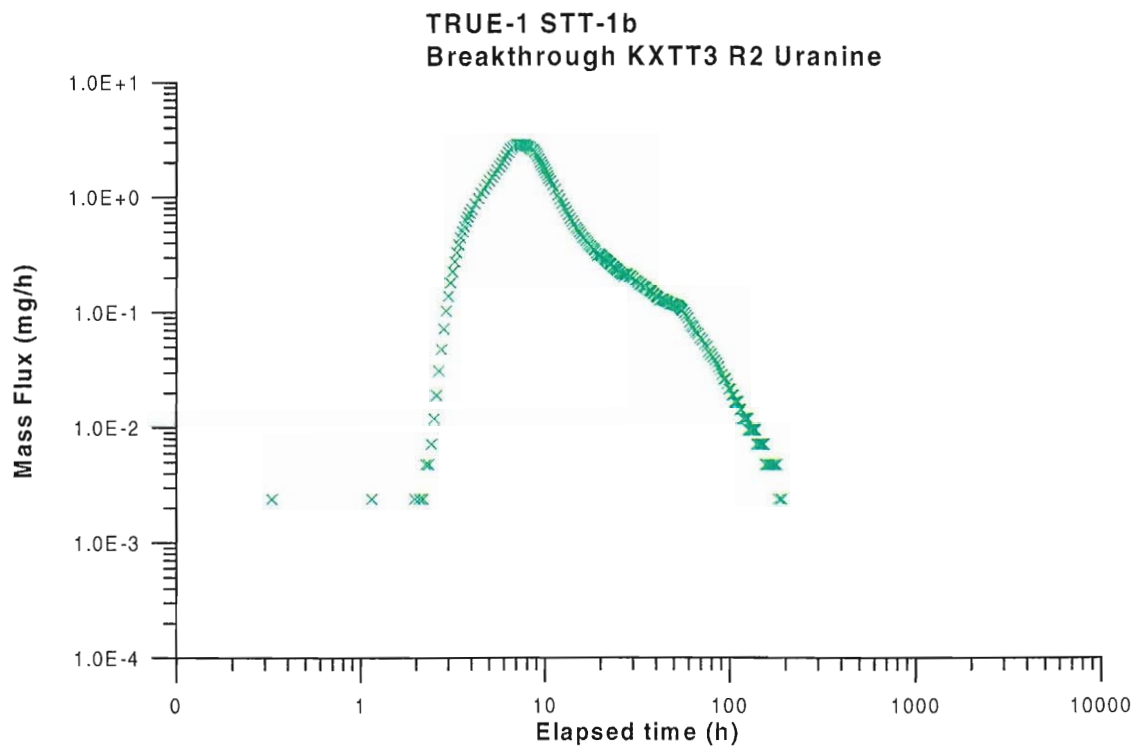
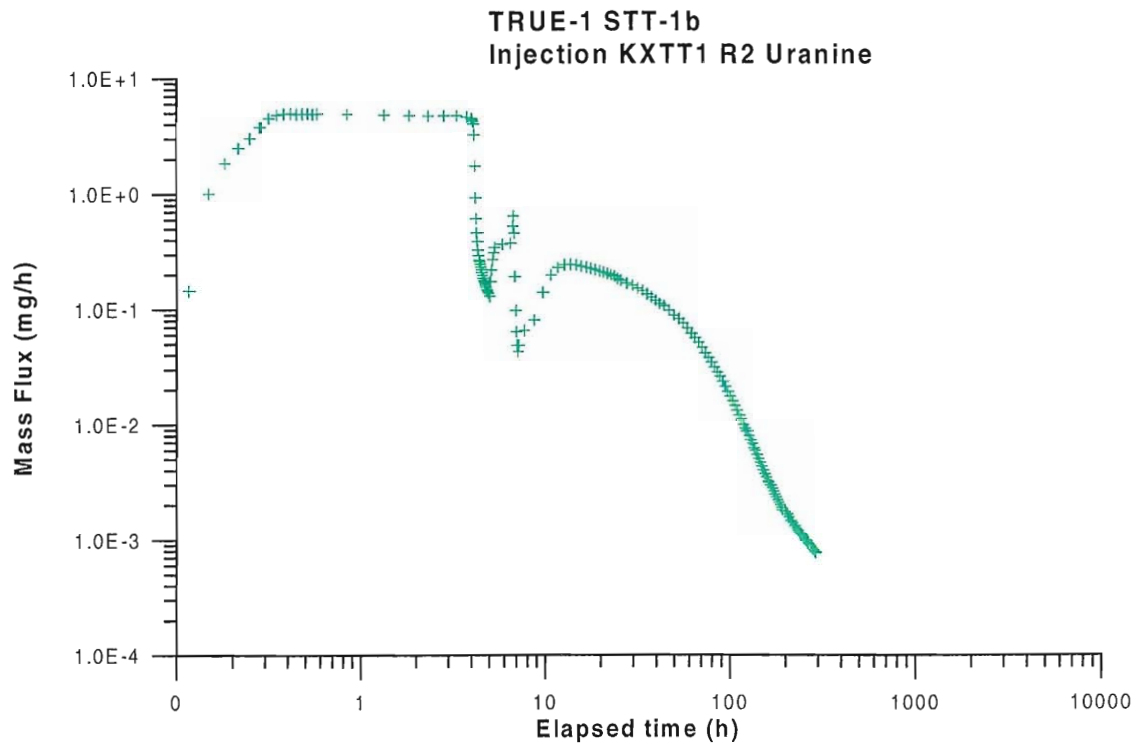
Van Genuchten M. Th, and Alves W. J, 1982. Analytical solutions of the one-dimensional convective-dispersive solute transport equation. U.S. Dep. Agric. Tech. Bull., 1661.

Winberg A (ed), 1996. First TRUE Stage - Tracer Retention Understanding Experiments. Descriptive structural-hydraulic models on block and detailed scales of the TRUE-1 site. Swedish Nuclear Fuel and Waste Management Company. Äspö Hard Rock Laboratory International Cooperation Report ICR 96-04.

Appendix A

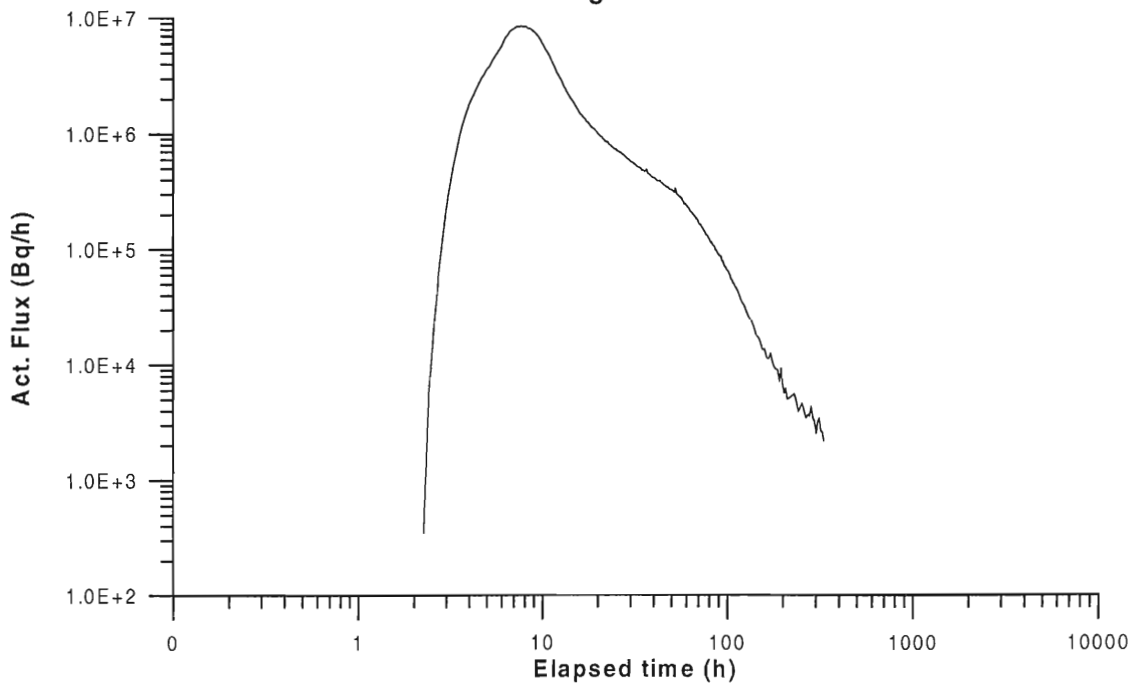
Tracer breakthrough data (log-log scale) and injection data (Uranine, log-log scale) from STT-1b and Cs-137 from STT-1.

A:1

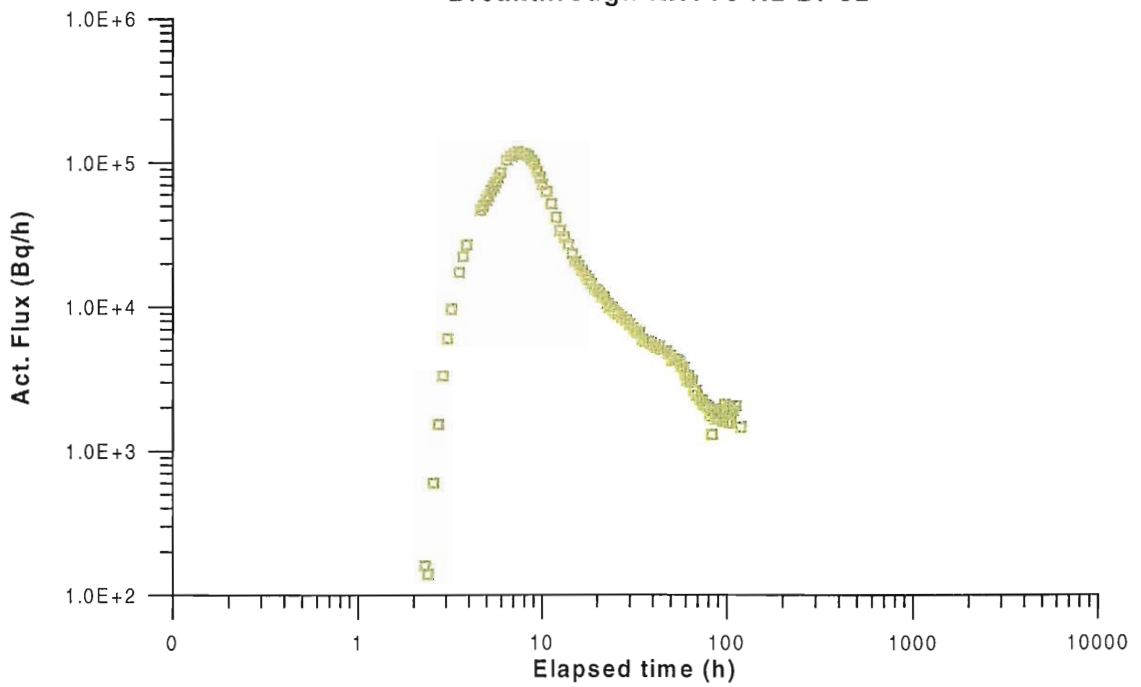


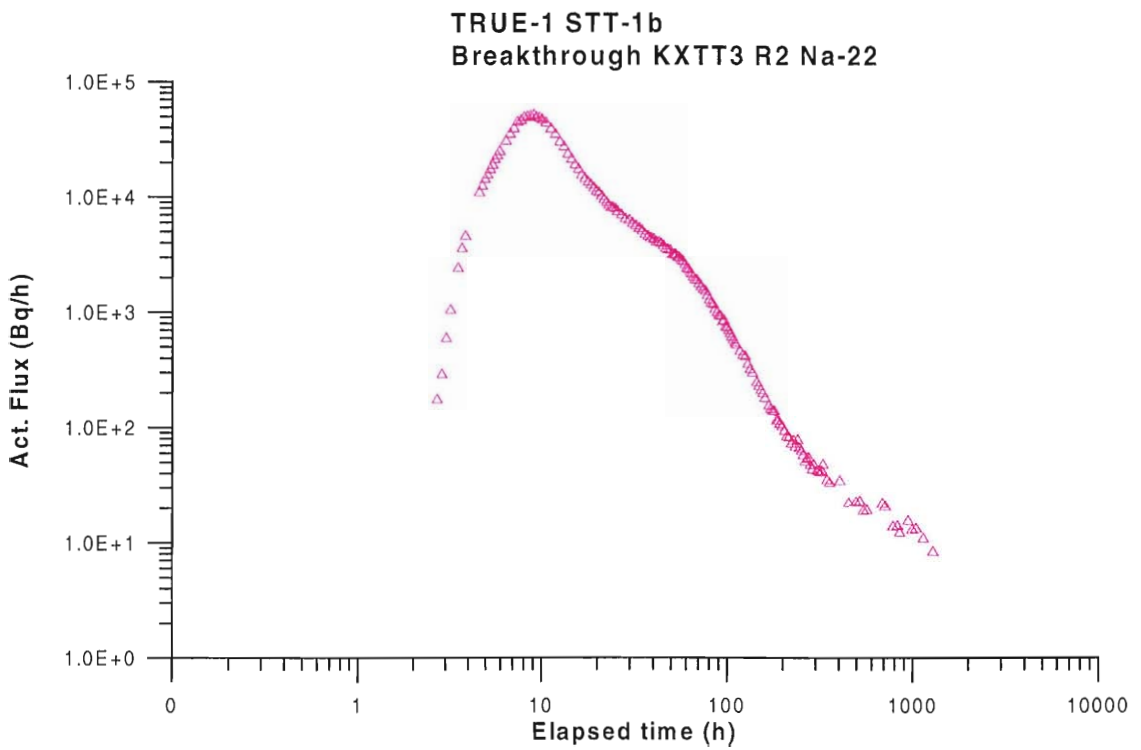
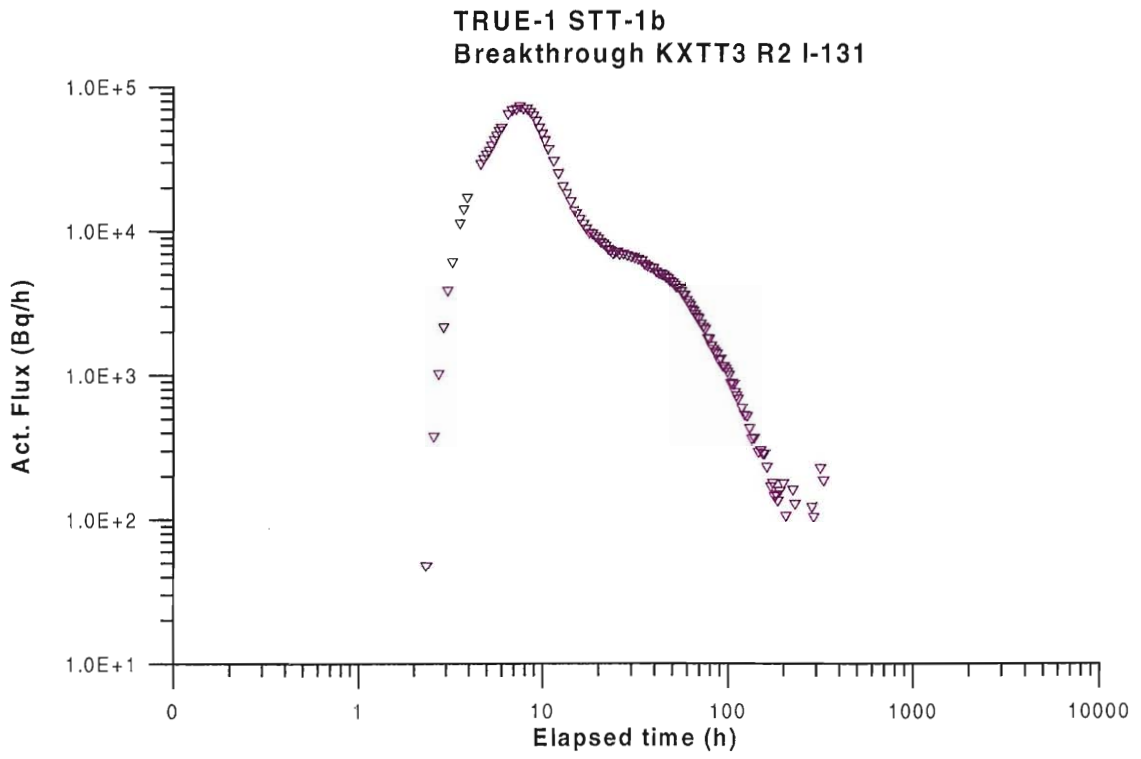
A:2

**TRUE-1 STT-1b
Breakthrough KXTT3 R2 Tritiated water**



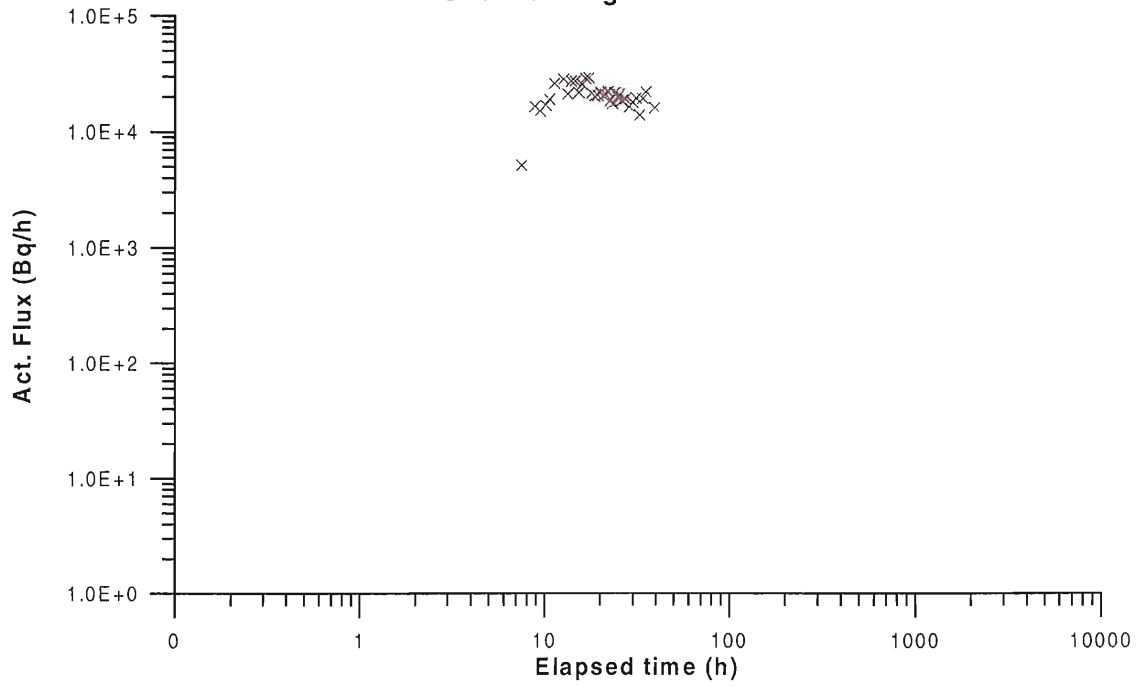
**TRUE-1 STT-1b
Breakthrough KXTT3 R2 Br-82**



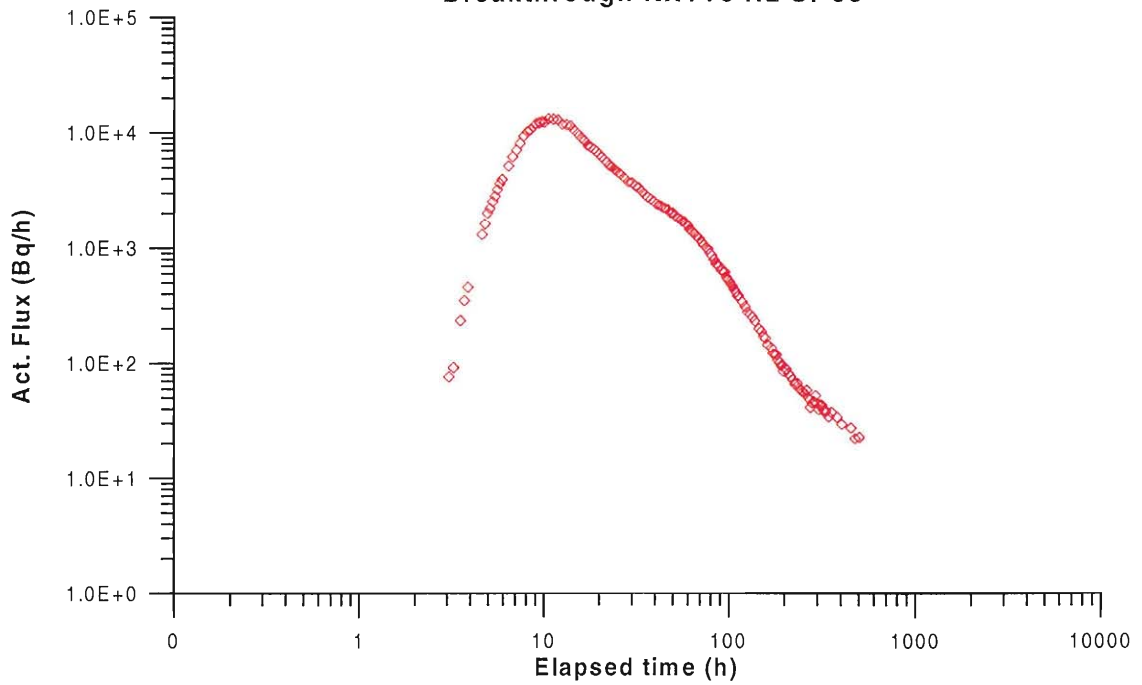


A:4

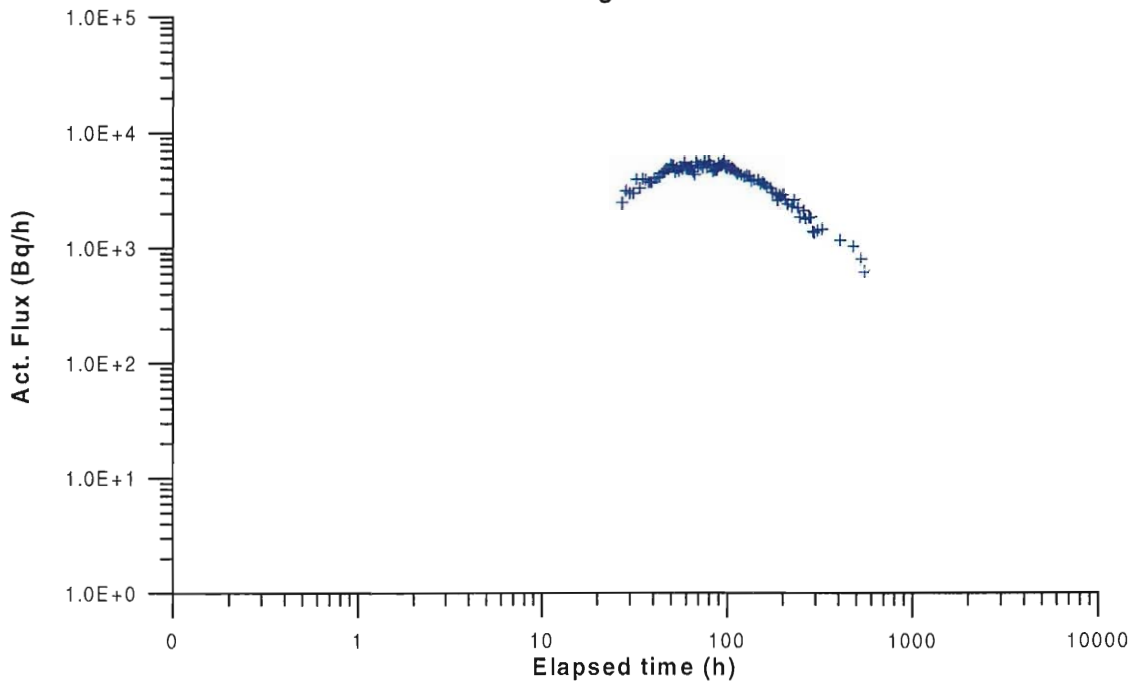
**TRUE-1 STT-1b
Breakthrough KXTT3 R2 K-42**



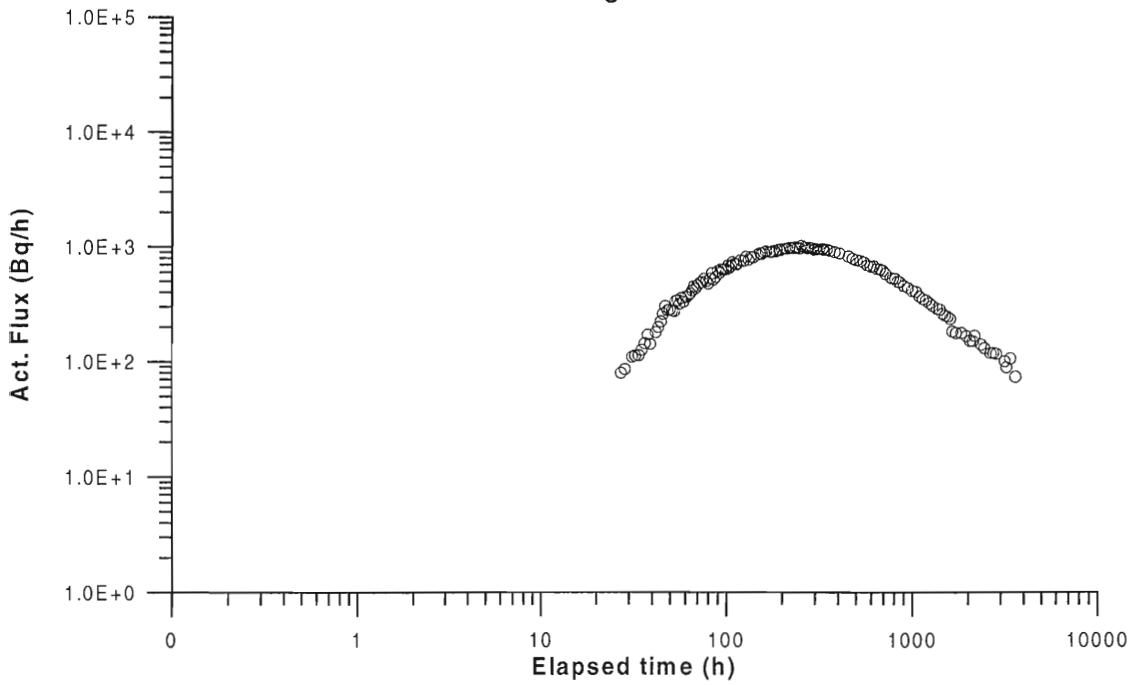
**TRUE-1 STT-1b
Breakthrough KXTT3 R2 Sr-85**



**TRUE-1 STT-1b
Breakthrough KXTT3 R2 Rb-86**



**TRUE-1 STT-1b
Breakthrough KXTT3 R2 Co-58**



TRUE-1 STT-1
Breakthrough KXTT3 R2 Cs-137

